Published in final edited form as:
J Med Chem. 2013 March 14; 56(5): 2045–2058. doi:10.1021/jm3017464.

Novel Triaryl Sulfonamide Derivatives as Selective Cannabinoid Receptor 2 Inverse Agonist and Osteoclast Inhibitor: Discovery, Optimization and Biological Evaluation

Peng Yang[1,2], **Liping Wang**[1,2], **Rentian Feng**[1,2], **Abdulrahman A. Almehizia**[1,2], **Qin Tong**[1,2], **Kyaw-Zeyar Myint**[1,2], **Qin Ouyang**[1,2], **Mohammed Hamed Alqarni**[1,2], **Lirong Wang**[1,2,3], and **Xiang-Qun Xie**[1,2,3,4,5,*]

[1]Department of Pharmaceutical Sciences and Computational Chemical Genomics Screening Center, School of Pharmacy, University of Pittsburgh, Pittsburgh, Pennsylvania 15260, United States

[2]Drug Discovery Institute, University of Pittsburgh, Pittsburgh, Pennsylvania 15260, United States

[3]Pittsburgh Chemical Methods and Library Development (CMLD) Center, University of Pittsburgh, Pittsburgh, Pennsylvania 15260, United States

[4]Department of Computational and Systems Biology, University of Pittsburgh, Pittsburgh, Pennsylvania 15260, United States

[5]Department of Structural Biology, University of Pittsburgh, Pittsburgh, Pennsylvania 15260, United States

Abstract

Cannabinoid receptors have gained more and more attention as drug targets for developing potential therapeutic ligands. Here, we report the discovery and optimization of triaryl sulfonamide as a novel series possessing significant CB_2 receptor affinity and selectivity. Four sets of triaryl ligands were designed, synthesized for further structural modifications, and led to the identification of eight compounds as potent and selective CB_2 inverse agonists with high binding affinity (CB_2 K_i < 10 nM). Especially, compound **57** exhibited the strongest binding affinity on CB_2 receptor (CB_2 K_i of 0.5 nM) and the best selectivity over CB_1 receptor (selectivity index of 2594). Importantly, **57** also showed potent inhibitory activity on osteoclast formation, and was confirmed its inhibition effects were not derived from its cytotoxicity by the cell viability assay. Finally, 3D QSAR studies confirmed our SAR findings that three bulky groups play an important role for CB_2 receptor binding affinity.

INTRODUCTION

Cannabinoids (CB) are a class of diverse chemical compounds, including the endocannabinoids (produced naturally in the body by humans and animals, such as **1** and **2**, Figure 1),[1–3] the phytocannabinoids (found in cannabis and some other plants, such as **3**),[4] and synthetic cannabinoids (produced chemically by humans, such as **4**)[5]. Before the 1980s, it was often speculated that cannabinoids produced their physiological and behavioral effects via nonspecific interaction with cell membranes, instead of interacting with specific membrane-bound receptors. The discovery of the first cannabinoid receptors in the 1980s helped to resolve this debate.[6] Two kinds of cannabinoid receptors have been found to date

*Corresponding Author. Xiang-Qun (Sean) Xie: Phone: +1-412-383-5276. Fax: +1-412-383-7436. xix15@pitt.edu.

and are termed CB_1 and CB_2. The CB_1 receptor is expressed predominantly in the brain (central receptor for cannabinoids),[6] and the CB_2 receptor in peripheral cells and tissues derived from the immune system (peripheral receptor for cannabinoids).[7]

The endocannabinoid system is known to play a key role in numerous biological processes and exhibits pharmacological effects in a large spectrum of diseases and disorders, such as pain,[8] autoimmune and neurodegenerative disorders,[9, 10] cancer,[11, 12] osteoporosis,[13] stoke,[14] inflammation[15] and fibrosis,[16] and cardiovascular and gastrointestinal disorders.[16–18] Thus, in the past several decades, investigations were aimed at designing new synthetic molecules that target cannabinoid receptors. But due to the unfavorable psychiatric side effects of CB_1 ligands,[19] the study of selective CB_2 ligands and their therapeutic potentials provoked medicinal chemist more and more interest. Several reviews,[20–24] including the latest review from our lab,[24] summarize the advances of new CB_2 ligands from literature and patents. The most notable CB_2-selective antagonists/inverse agonists are the diarylpyrazole **5** (SR144528),[25] and 6-iodopravadoline **6** (AM 630).[26] Both compounds bind with much higher affinity to CB_2 than to CB_1 receptors, and have been extensively used as standards to measure the specificity of various cannabinoid agonists. Among these potential and selective CB_2 ligands, **7** (JWH-133)[27] is a representative agonist for the non-psychoactive CB_2 receptor and hence devoid of any psychoactive side effects or abuse potential, which also showed good activity to decrease experimental colitis[28] and dose-dependently inhibited intravenous cocaine self-administration, cocaine-enhanced locomotion, and cocaine-enhanced accumbens extracellular dopamine.[29] Another two notable CB_2-selective inverse agonists are **8** (Sch225336)[30] and **9** (JTE-907)[31], which have immunomodulatory properties against inflammatory disorders. Obviously, more and more evidence indicates CB_2 receptor is an attractive and promising target for developing potentially therapeutic ligands.

Here, we report the identification, optimization and therapeutic potential of a novel class of CB_2 selective inverse agonists. Within an *in vitro* high-throughput screening research program to discover novel CB_2-selective ligands, compound **10** *N*-(4-chlorophenethyl)-4-methyl-*N*-tosylbenzenesulfonamide was identified as a novel chemotype with selective CB_2 activity (CB_2 *K*i = 192 nM, selectivity index of 26-fold, Figure 2). On the basis of this promising result, we considered **10** as a lead compound and conducted further medicinal chemistry structure-activity relationship (SAR) studies. Four series of compounds were designed, synthesized and tested in competition binding activities and effects on both CB_2 and CB_1 receptors to define their structure-activity relationships. The representative compounds were also examined in cAMP assays on hCB_2 CHO cells, with the aim of evaluating their functionality. Our systematic studies led to the identification of eight new derivatives (CB_2 *K*i < 10 nM) as novel CB_2 inverse agonists with improved CB_2 binding affinity and selectivity. Importantly, some showed promising inhibition activity to osteoclast cells without any sign of toxicity on osteoclast precursor.

RESULTS AND DISCUSSION

Chemistry

The synthetic routes to obtain the target triaryl sulfonamide derivatives are outlined in Scheme 1. The commercially available 4-(diethylamino)benzaldehyde was reacted with adamantan-1-amine in methanol to give **11**, which, when treated with $NaBH_4$ gave the secondary amine **12**. Finally, the coupling reaction between intermediate **12** and selected acyl chloride or sulfonyl chloride yielded the corresponding compounds **20**–**30**. Taking heptan-1-amine, *p*-toluidine or 4-chloroaniline as the starting material, the synthesis of target compounds **31**–**44**, **45**–**53** and **54**–**63** was accomplished using a procedure similar to that

utilized for preparing compounds **20**–**30**. The target compounds were purified by flash column chromatography.

Pharmacology and SAR Analysis

Taking **10** as the lead compound, we have carried out medicinal chemistry modification, designed and synthesized 46 analogues for further SAR studies. The CB_2 binding affinities of these 46 derivatives were determined by performing [^{3}H]CP-55,940 radioligand competition binding assays. The CB_1 binding assay was also conducted for those compounds with high CB_2 receptor binding potency (K_i < 200 nM). CB_2 selective ligand **1** (SR144528, CB_2 inverse agonist) and CB_1 ligand **19** (SR141716, CB_1 inverse agonist)[32] were used as positive controls along with tested compounds in bioassays experiments. Among 46 novel triaryl sulfonamide derivatives, 21 compounds displayed high affinity for the CB_2 receptors (K_i < 100 nM) and 10 compounds showed better affinity for the CB_2 receptors (K_i < 10 nM). The chemical structures, binding activities, and selectivity index are summarized in Tables 1–4.

To get more potent compounds with higher CB_2 affinity and selectivity, we introduced different functional groups to compound **10**. Our SAR strategies to modify the lead compound included replacing 4-chlorophenethyl with 4-(diethylamino)benzyl, which has been confirmed as a good fragment for CB_2 ligands in our previous studies[33], keeping one of the sulfonyl groups, and replacing another *p*-toluenesulfonyl with adamantyl, heptyl, *p*-tolyl or *p*-chlorobenzyl.

Removal of one *p*-toluenesulfonyl group (compound **12**, CB_2 K_i = 19950 nM, Table 1) dramatically decreased the CB_2 binding activity, which indicated these three hydrophobic groups (ring A, B and C, Figure 2) may be essential for the activity.

Compared with lead compound **10**, replacing 4-chlorophenethyl (ring C) and one p-toluenesulfonyl (ring A) with 4-(diethylamino)benzyl and adamantyl (compound **24**, CB_2 K_i = 47 nM, selectivity index = 425) dramatically increased the CB_2 binding activity and selectivity. The result indicated this is a good direction for further modification. Compared to our previous reported biamide scaffold,[32] this new triaryl sulfonamide scaffold is more stable. In the meanwhile, we have several compounds which replaced both arylsulfonamide groups in our high-throughput screening, but the results were not so good (data not shown). So the SAR study was first focused on another *p*-toluenesulfonyl group (ring B). An initial set of 11 compounds (**20**–**30**, Table 1) was synthesized by replacing *p*-toluenesulfonyl with different sulfonyl or acyl groups. Compared with compound **24**, removal of the methyl group (compound **20**, CB_2 K_i = 84 nM, selectivity index = 130) slightly decreased the CB_2 binding activity and selectivity. Replacing the methyl group with fluorine (compound **21**, CB_2 K_i = 25 nM, selectivity index = 170) increased the activity but decreased the selectivity. While replacing the methyl group with chlorine (compound **22**, CB_2 K_i = 173 nM, selectivity index = 11) decreased both the activity and the selectivity. To explore the effect of the substituent size on CB_2 binding activity, we introduced two bigger groups methoxyl (compound **23**) and *i*-propyl (compound **26**), but both of them showed decreased activity and selectivity. Interestingly, moving the methyl group to the meta position gave a promising compound **25** (Figure 3) with increased activity and selectivity (CB_2 K_i = 25 nM, selectivity index = 432). Furthermore, we replaced the *p*-toluenesulfonyl group with different acyl groups. Replacing *p*-toluenesulfonyl with cyclohexanecarbonyl gave another promising compound **27** (CB_2 K_i = 35 nM, selectivity index = 571). And replacing *p*-toluenesulfonyl with phenylacetyl or 4-chlorophenylacetyl showed similar results (compound **29**, CB_2 K_i = 38 nM, selectivity index = 526; compound **30**, CB_2 K_i = 60 nM, selectivity index of > 333). While replacing *p*-toluenesulfonyl with octanoyl (compound **28**,

CB_2 K_i = 638 nM) showed dramatically decreased activity. These results (compounds **27**–**30**) indicated the sulfonyl group may not be essential for the CB_2 binding activity, but a bulky ring group plays an important role to keep better binding affinity.

Keeping 4-(diethylamino)benzyl group, the SAR studies were extended by replacement of two *p*-toluenesulfonyl groups with heptyl and a series of different sulfonyl or acyl groups to evaluate the effect of a long chain substituent (compounds **31**–**44**, Table 2). Unfortunately, all of these compounds showed dramatically decreased CB_2 binding activity (CB_2 K_i of > 212 nM). These results further confirmed that three bulky rings may be essential for the CB_2 binding activity of triaryl sulfonamide derivatives.

Since three bulky ring groups are important for good CB_2 binding activity and selectivity, we kept the 4-(diethylamino)benzyl group, replaced two *p*-toluenesulfonyl groups with *p*-tolyl or *p*-chlorobenzyl and a series of different sulfonyl or acyl groups to further evaluate the effect on receptor affinity and selectivity of structural modifications on the benzene ring. Two series of compounds (**17**, **45**–**53**, Table 3; and **54**–**63**, Table 4) were synthesized.

To keep three bulky ring groups and get more potent compounds with good binding affinity and selectivity, we first replaced one *p*-toluenesulfonyl group with *p*-chlorobenzyl (compound **49**, CB_2 K_i = 37 nM, selectivity index = 3.7). This result indicated that the introduction of *p*-chlorobenzyl may enhance the affinity on CB_2 receptor, but lost the selectivity. While compound **17** bearing only two bulky ring groups (CB_2 K_i = 6741 nM) showed dramatically decreased affinity at the CB_2 receptor, suggesting the important role of three bulky ring groups in this series compounds, as confirmed above. Compared with compound **49**, removing the methyl group from *p*-toluenesulfonyl (compound **45**, CB_2 K_i = 20 nM, selectivity index = 88) improved both the binding affinity on the CB_2 receptor and the selectivity over the CB_1 receptor. Replacing methyl with fluorine (compound **46**, CB_2 K_i = 73 nM, selectivity index = 15) did not lead to significant effects on affinity and selectivity. While better results were obtained with compound **47** (CB_2 K_i = 36 nM, selectivity index = 183), in which the methyl group was replaced by chlorine, showing similar binding affinity but increased selectivity. Interestingly, replacing methyl with methoxyl (compound **48**, CB_2 K_i = 14 nM, selectivity index of > 1428, Figure 3) showed high affinity and remarkable selectivity at the CB_2 receptor. Similarly to compounds **25** and **26**, moving the methyl group to the meta position gave a promising compound **50** with greatly increased affinity and selectivity (CB_2 K_i = 2.8 nM, selectivity index = 309, Figure 3), and introduction of a bigger group isopropyl (compound **51**, CB_2 K_i = 222 nM) caused a dramatic loss of affinity for the CB_2 receptor. While differently from compounds **29** and **27**, replacing *p*-toluenesulfonyl with aromatic 4-chlorophenylacetyl (compound **52**, CB_2 K_i = 136 nM) or nonaromatic cyclohexanecarbonyl (compound **53**, CB_2 K_i = 164 nM) showed slightly decreased CB_2 binding affinity.

Besides *p*-chlorobenzyl, we also replaced one *p*-toluenesulfonyl group with *p*-tolyl and discovered a series of promising compounds with greatly improved binding affinity (compounds **54**–**60**, CB_2 K_i of < 10 nM, Table 4). As seen with the *p*-chlorobenzyl series, compound **58** (CB_2 K_i = 5.4 nM, selectivity index = 80) shows greater affinity and selectivity for the CB_2 receptor than the lead compound **10**. Compared with compound **58**, removing methyl (compound **54**, CB_2 K_i = 3.4 nM, selectivity index = 151) or replacing methyl with fluorine (compound **55**, CB_2 K_i = 5.6 nM, selectivity index = 153) or chlorine (compound **56**, CB_2 K_i = 3.0 nM, selectivity index = 137, Figure 3) resulted in similar affinity and slightly increased selectivity for the CB_2 and CB_1 receptors, suggesting a variety of substituents on this position was tolerated. While moving the methyl group to the meta position (compound **59**, CB_2 K_i = 5.8 nM, selectivity index = 37) caused a slight decrease of affinity and selectivity for the CB_2 receptor. In contrast, replacing methyl with a

bigger group isopropyl (compound **60**, CB_2 K_i = 4.3 nM, selectivity index = 782) led to significant improvement of selectivity with similar CB_2 binding affinity. In particular, introduction of methoxyl proved to have the greatest affinity for the CB_2 receptor in this series (compound **57**, CB_2 K_i = 0.5 nM, Figure 3), with an excellent selectivity (selectivity index = 2594). While replacing *p*-toluenesulfonyl with substituted acyl (compounds **61**–**63**, Table 4) led to a significant reduction in affinity and selectivity. Together, these compounds indicate that *p*-toluenesulfonyl and *p*-tolyl are a good combination to improve affinity and selectivity for the CB_2 receptor.

Functional Activity at CB_2 Receptors in Vitro

CB_2 functional activities of triaryl sulfonamide derivatives were investigated by using a cell-based LANCE cAMP assay, which is a useful method to distinguish between agonists, inverse agonists and neutral antagonists. Cellular bioassay was carried out to measure the functional activities of the CB_2 selective compounds, as previously described[34]. Briefly, the cell-based LANCE cAMP assays were performed on 384-well plates using CHO cells stably expressing the CB_2 receptors in the presence of phosphodiesterase inhibitor RO20-1724 and adenyl cyclase activator forskolin. As shown in Figure 4, reduction of the LANCE signal occurred with increasing concentrations of compounds **21**, **48**, **54**, **57**, and **5**. These ligands acted as inverse agonists, indicated by increasing forskolin-induced cAMP production, with EC_{50} values of 268.4 ± 14.5 nM, 16.4 ± 2.84 nM, 608.6 ± 6.06 nM, 42.7 ± 1.35 nM, and 153.8 ± 5.58 nM, respectively. Such a phenomenon was not observed with agonists CP55940 and HU308, which inhibited cAMP production with EC_{50} values of 47.1 ± 3.43 nM and 83.8 ± 5.63 nM, respectively. The results clearly indicated that four top compounds (**21**, **48**, **54**, and **57**) indeed behaved as inverse agonists.

Osteoclast Formation Bioactivity

Osteoporosis is a degenerative skeletal disease and a serious public health problem, particularly among in postmenopausal women and older men, which is characterized by reduced bone mass and increased risk of fractures. Scientists now speculate that the main physiologic involvement of CB_2 receptors is to maintain bone remodeling at balance, thus protecting the skeleton against age-related bone loss,[35] leading more experts to believe that cannabinoids may be a promising target novel target for anti-osteoporotic drug development.[13] On the basis of binding affinity, selectivity, functionality, and druglikeness studies above, three compounds were selected as top candidates to be evaluated against RANKL-induced osteoclast differentiation on RAW 264.7 cells. RAW 264.7 is a mouse monocytic cell line that is used as a standard osteoclast differentiation model. As shown in Figure 5, we tested the effect of these most promising CB_2 ligands on osteoclast (OCL) formation using RAW 264.7 cells.[36] Each ligand tested induced a concentration-dependent inhibition of osteoclastogenesis and all of these three compounds showed strong potency in suppressing OCL formation at 10 μM, with inhibition rates of > 95%. Compounds **48** and **57** also showed good inhibition activity at low dose of 1 μM (Figure 5). Meanwhile, these results indicated that the inhibition activities are consistent with the CB_2 binding affinities. Especially, compound **57** showed the strongest inhibition activity, with inhibition rates of 46%, 97%, and 100% at 0.1, 1, and 10 μM, respectively.

Cytotoxicity Studies of Compounds 48 and 57 Using RAW 264.7 Cells

Our newly discovered compounds **48** and **57** showed promising inhibition effects on osteoclastogenesis. To examine whether the impaired osteoclastogenesis in the presence of compounds **48** and **57** is due to the decrease in viability of the precursor cells, we investigated the cytotoxicity profile of these two compounds upon osteoclast precursors RAW 264.7 by standard MTT assay. First, RAW 264.7 cells were plated on 96-well plates

and incubated with compounds **48** and **57** for 3 days. The percentage of cell survival was determined with the MTT assay. The results indicated that the cell viability was not significantly affected in comparing with the vehicle control group at 1.25 and 2.5 μM, and only some effects on cell viability were observed at high concentrations of 5 and 10 μM (Figure 6). The best compound **57** did not show any cytotoxic effects at 1.25 μM (97% inhibition rate at 1 μM), and only slight effect on cell viability were observed at high concentration of 5 μM. The results suggested that our compounds possess favorable therapeutic indexes and the effects of **57** on osteoclast differentiation were not derived from its cytotoxicity.

3D QSAR Studies of New CB_2 Ligands

3D QSAR studies were carried out for the synthesized analogues to correlate structural and experimental data for further SAR studies by using our published protocol[37, 38]. Compound **57** was chosen as a template compound for QSAR studies given its high CB_2 affinity, selectivity, and high inhibition of osteoclastgenesis. In this study, 3D QSAR model was built using the Comparative Molecular Field Analysis (CoMFA) method, which is the most commonly used 3D QSAR technique in lead optimization and drug discovery. Molecular dynamic and molecular mechanics (MD/MM) simulations were carried out based on our published protocol[39] to search for preferred conformations of compound **57**. MD simulations were performed to generate four families of conformations. These conformations were compared to the docking pose that resulted from molecular docking simulations using our in house 3D CB_2 receptor model.[40] One of the conformations that was closest to the docking pose conformation was used as a template conformation. All compounds from the training set (Table 5) and the test set (Table 6) were aligned to the preferred conformer of compound **57**. The final alignment of the training and test sets are depicted in Figure 7A, B.

Subsequently, partial least squares (PLS) analysis was performed using leave-one-out cross-validation (LOOCV), which is a cross-validation method in which each training sample is left out iteratively and systematically in each training round to determine the optimal number of components and the predictive ability of each CoMFA model was determined by the cross validated r^2:

$$r_{cv}^2 = (SD - PRESS)/SD$$

where SD is the sum of the squared deviations of between the biological activity of the molecules and PRESS is the sum of all the squared deviations between the actual and predicted activity values. The PLS analysis showed that the optimal number of components was 4 and the r_{cv}^2 was 0.577, which was in the range of generally accepted criterion for statistical validity. Non-cross-validated PLS analysis was then performed and the r^2 was 0.969 with a standard error of estimate (SEE) of 0.201. Field contribution of steric and electrostatic fields accounts for 0.502 and 0.498, respectively. Such results indicate that the trained CoMFA model successfully correlates the structural information of synthesized analogs to their CB_2 receptor affinity values. To further evaluate the generated CoMFA model's generalization ability, the model was used to predict the binding affinity values of test set compounds, which were not part of the training set molecules. The correlation coefficient (r_2) for the test set was 0.947, which demonstrated that the CoMFA model had a good generalization performance on the test set molecules. The experimental activities, predicted activities and their residues of the 33 training set molecules and 12 test set molecules are listed in Tables 5 and 6. The predicted p*K*i values are close to the experimental p*K*i values for molecules in both the training set and test set. The regression lines of the experimental and predicted activity of the training and test sets molecules are shown in Figures 8 and 9. The linearity of the plot indicates a good correlation and the

ability of the developed CoMFA model to predict CB_2 receptor binding affinities of the synthesized analogues.

The steric and electrostatic contour map for the CoMFA model was then generated in order to predict the favorable and unfavorable regions of the new derivatives for CB_2 receptor binding activity. CoMFA contour maps depict the color coded steric and electrostatic regions around the molecules that associate with ligand biological activities. Green regions indicate favorable steric interactions that enhance binding affinity, while a yellow region indicates unfavorable steric interactions. The red and blue contours reflect whether electropositive or electronegative substituents are favored at a particular position. As shown in Figure 7C, there is a large sterically preferable region near rings A and B, which means the introduction of a bulky hydrophobic group or an aromatic ring in this area will enhance the CB_2 binding affinity. This is consistent with the structural modification of compounds **50** and **59**, which have a methyl group on the meta position. And this is also consistent with the results of compounds **31**–**44** bearing an alkyl chain as ring B (CB_2 K_i of > 212 nM) and **54**–**60** bearing a bulky group as ring B (CB_2 K_i of < 6 nM), which indicates these bulky groups play an important role to enhance the CB_2 binding affinity. On the contrary, steric interactions are not preferred near the para position of ring A as highlighted by a yellow region. This matches the results of compounds **26**, **35**, and **51** with isopropyl, isopropoxyl, and isopropyl, respectively, which showed lower or complete loss of CB_2 binding activities. On the other hand, electronegative interactions are preferred near the para position of ring B as highlighted as a blue region. However, electropositive interactions are preferred beside the ortho position of ring C as highlighted by a red region, which is consistent with our previous CoMFA studies.[33] In conclusion, our CoMFA studies corroborate our SAR results that these bulky groups play an important role to keep good CB_2 binding activity and selectivity.

CONLUSION

We have discovered *N*-(4-(diethylamino)benzyl)-4-methoxy-*N*-(p-tolyl)benzenesulfonamide as a novel series of CB_2 ligands possessing high binding affinity to cannabinoid CB_2 receptor. To increase selectivity and avoid or reduce potential CB_1-associated CNS adverse effects, we designed, synthesized 46 analogues, and evaluated their binding affinity and selectivity on CB_2/CB_1 receptors for further SAR studies. Among them, eight compounds exhibited high binding affinity on CB_2 receptor (CB_2 K_i of < 10 nM) and good selectivity over CB_1 receptor (CB_1/CB_2 of 37- to 2594-fold). Top four compounds were measured in functional assays, revealing that the novel series behaves as CB_2 receptor inverse agonists. Compounds **25**, **48**, and **57** showed potent inhibitory activity on RANKL-induced osteoclast formation. Especially, **57** showed the strongest inhibition activity even at low concentration of 0.1 μM. The cell viability test of **57** on RAW 264.7 showed very low cytotoxic effects, which confirmed its inhibition effects on osteoclast were not derived from its cytotoxicity. 3D QSAR studies also confirmed our SAR findings that three bulky groups are important for CB_2 receptor activity. Overall, this novel series of compounds offers an attractive starting point for further optimization and represents a promising lead for the development of a new class of antiosteoporosis agents.

EXPERIMENTAL SECTION

Chemistry

All reagents were purchased from commercial sources and used without further purification. Analytical thin-layer chromatography (TLC) was performed on SiO_2 plates on alumina. Visualization was accomplished by UV irradiation at 254 nm. Flash column chromatography was performed using the Biotage Isolera flash purification system with

SiO_2 60 (particle size 0.040–0.055 mm, 230–400 mesh). ^1H NMR was recorded on a Bruker 400 MHz spectrometer. Splitting patterns are indicated as follows: s, singlet; d, doublet; t, triplet; m, multiplet; br, broad peak. Purity of all final derivatives for biological testing was confirmed to be > 95% as determined using the following conditions: a Shimadzu HPLC instrument with a Hamilton reversed phase column (HxSil, C18, 3 μm, 2.1 mm × 50 mm (H2)); eluent A consisting of 5% CH_3CN in H_2O; eluent B consisting of 90% CH_3CN in H_2O; flow rate of 0.2 mL/min; UV detection, 254 and 214 nm.

General Procedure for Synthesis of Secondary Amine Building Blocks

(3s,5s,7s,E)-N-(4-(Diethylamino)benzylidene)adamantan-1-amine (11)—(3s,5s,7s)-adamantan-1-amine hydrochloride (3.75 g, 20 mmol) was added slowly to a solution of 4-(diethylamino)benzaldehyde and methanol (50 mL). The mixture was stirred and refluxed for 12 h. The reaction mixture was cooled to room temperature and the solvent was removed by evaporation in vacuum to give the crude compound **11**, which was used to the next step without further purification.

(3s,5s,7s)-N-(4-(Diethylamino)benzyl)adamantan-1-amine (12)—The crude compound **11** was dissolved in methanol (50 mL) and $NaBH_4$ (1.14 g, 30 mmol) was added. The mixture was continued to stir for 12 h at room temperature. The reaction solution was poured into water and extracted with EA. The combined organic layers were washed with water and brine, and then dried over Na_2SO_4. The mixture was filtered and the solvent was evaporated in vacuum. The residue was purified by flash chromatography on silica gel to obtain **12** (5.8 g, 88%). ^1H NMR (400 MHz, DMSO-d_6) δ 7.13 (d, J = 8.0 Hz, 2H), 6.62 (d, J = 8.0 Hz, 2H), 3.65 (bs, 1H), 3.42–3.48 (m, 2H), 3.28–3.39 (m, 4H), 2.05–2.07 (m, 3H), 1.58–1.71 (m, 12H), 1.07 (t, J = 6.8 Hz, 6H). LC–MS (ESI): *m/z* 313.2 $(M + H)^+$.

4-(((4-Chlorophenyl)amino)methyl)-N,N-diethylaniline (17)—Yield: 78%. ^1H NMR (400 MHz, DMSO-d_6) δ 7.03–7.14 (m, 4H), 6.56–6.62 (m, 4H), 6.19–6.22 (m, 1H), 4.06–4.07 (m, 2H), 3.27–3.34 (m, 4H), 1.06 (t, J = 6.8 Hz, 3H). LC-MS (ESI): *m/z* 289.0 $(M + H)^+$.

General Procedure for the Coupling Reaction between Secondary Amine and Acyl Chloride or Sulfonic Chloride

N-((3s,5s,7s)-Adamantan-1-yl)-N-(4-(diethylamino)benzyl)benzenesulfonamide (20)—The intermediate **12** (328 mg, 1.0 mmol) in dichloromethane (DCM, 5 mL) was chilled in ice with the exclusion of moisture and them triethylamine (122 mg, 1.2 mmol) was added to it. The resulting solution was treated dropwise under stirring with benzenesulfonyl chloride (177 mg, 1.0 mmol) also dissolved in DCM over 30 min at 0 °C and them left overnight at room temperature. The reaction solution was poured into water and extracted with EA. The combined organic layers were washed with water and brine, and then dried over Na_2SO_4. The mixture was filtered and the solvent was evaporated in vacuum. The residue was purified by flash chromatography on silica gel to obtain **20** (400 mg, 85%). ^1H NMR (400 MHz, DMSO-d_6) δ 7.13 (d, J = 8.0 Hz, 2H), 6.62 (d, J = 8.0 Hz, 2H), 3.65 (bs, 1H), 3.42–3.48 (m, 2H), 3.28–3.39 (m, 4H), 2.05–2.07 (m, 3H), 1.58–1.71 (m, 12H), 1.07 (t, J = 6.8 Hz, 6H). LC–MS (ESI): *m/z* 453.1 $(M + H)^+$.

N-((3s,5s,7s)-Adamantan-1-yl)-N-(4-(diethylamino)benzyl)-4-fluorobenzenesulfonamide (21)—Yield: 87%. ^1H NMR (400 MHz, DMSO-d_6) δ 7.87–7.89 (m, 2H), 7.38–7.43 (m, 2H), 7.21 (d, J = 8.8 Hz, 2H), 6.64 (d, J = 8.8 Hz, 2H), 4.59 (s, 2H), 3.29–3.36 (m, 4H), 1.88–1.93 (m, 9H), 1.42–1.51 (m, 6H), 1.07–1.10 (m, 6H). LC–MS (ESI): *m/z* 471.0 $(M + H)^+$.

N-((3s,5s,7s)-Adamantan-1-yl)-4-chloro-N-(4-(diethylamino)benzyl)benzenesulfonamide (22)—Yield: 92%. ^{1}H NMR (400 MHz, DMSO-d_6) δ 7.83 (d, J = 8.4 Hz, 2H), 7.64 (d, J = 8.8 Hz, 2H), 7.21 (d, J = 8.8 Hz, 2H), 6.65 (d, J = 8.8 Hz, 2H), 4.60 (s, 2H), 3.29–3.37 (m, 4H), 1.88–1.93 (m, 9H), 1.42–1.51 (m, 6H), 1.07–1.11 (m, 6H). LC–MS (ESI): *m/z* 487.1 $(M + H)^+$.

N-((3r)-Adamantan-1-yl)-N-(4-(diethylamino)benzyl)-4-methoxybenzenesulfonamide (23)—Yield: 89%. ^{1}H NMR (400 MHz, DMSO-d_6) δ 7.72–7.74 (m, 2H), 7.21 (d, J = 8.8 Hz, 2H), 7.07–7.10 (m, 2H), 6.64 (d, J = 8.8 Hz, 2H), 4.56 (s, 2H), 3.85 (s, 3H), 3.29–3.33 (m, 4H), 1.87–1.92 (m, 9H), 1.42–1.50 (m, 6H), 1.07–1.10 (m, 6H). LC–MS (ESI): *m/z* 483.0 $(M + H)^+$.

N-((3s,5s,7s)-Adamantan-1-yl)-N-(4-(diethylamino)benzyl)-4-methylbenzenesulfonamide (24)—Yield: 86%. ^{1}H NMR (400 MHz, DMSO-d_6) δ 7.70 (d, J = 8.4 Hz, 2H), 7.38 (d, J = 8.0 Hz, 2H), 7.23 (d, J = 8.8 Hz, 2H), 6.65 (d, J = 8.8 Hz, 2H), 4.59 (s, 2H), 3.30–3.42 (m, 4H), 2.40 (s, 3H), 1.87–1.92 (m, 9H), 1.40–1.50 (m, 6H), 1.03–1.12 (m, 6H). LC–MS (ESI): *m/z* 467.2 $(M + H)^+$.

N-((3s,5s,7s)-Adamantan-1-yl)-N-(4-(diethylamino)benzyl)-3-methylbenzenesulfonamide (25)—Yield: 84%. ^{1}H NMR (400 MHz, DMSO-d_6) δ 7.58–7.62 (m, 2H), 7.42–7.48 (m, 2H), 7.23 (d, J = 8.4 Hz, 2H), 6.65 (d, J = 8.4 Hz, 2H), 4.60 (s, 2H), 3.30–3.34 (m, 4H), 2.39 (s, 3H), 1.87–1.92 (m, 9H), 1.41–1.50 (m, 6H), 1.07–1.11 (m, 6H). LC–MS (ESI): *m/z* 467.1 $(M + H)^+$.

N-((3s,5s,7s)-Adamantan-1-yl)-N-(4-(diethylamino)benzyl)-4-isopropylbenzenesulfonamide (26)—Yield: 71%. ^{1}H NMR (400 MHz, DMSO-d_6) δ 7.72 (d, J = 8.0 Hz, 2H), 7.44 (d, J = 8.0 Hz, 2H), 7.20 (d, J = 8.8 Hz, 2H), 6.64 (d, J = 8.8 Hz, 2H), 4.57 (s, 2H), 3.27–3.29 (m, 4H), 2.97–3.01 (m, 1H), 1.89–1.92 (m, 9H), 1.41–1.51 (m, 6H), 1.19–1.24 (m, 6H), 1.08–1.10 (m, 6H). LC–MS (ESI): *m/z* 495.2 $(M + H)^+$.

N-((3s,5s,7s)-Adamantan-1-yl)-N-(4-(diethylamino)benzyl)cyclohexanecarboxamide (27)—Yield: 89%. ^{1}H NMR (400 MHz, $CDCl_3$) δ 7.03 (d, J = 8.8 Hz, 2H), 6.68 (d, J = 8.8 Hz, 2H), 4.49 (s, 2H), 3.35–3.40 (m, 4H), 2.36–2.42 (m, 1H), 2.22 (d, J = 2.4 Hz, 6H), 2.03–2.07 (m, 3H), 1.54–1.76 (m, 14H), 1.18–1.21 (m, 8H). LC–MS (ESI): *m/z* 423.5 $(M + H)^+$.

N-((3s,5s,7s)-Adamantan-1-yl)-N-(4-(diethylamino)benzyl)octanamide (28)—Yield: 81%. ^{1}H NMR (400 MHz, $CDCl_3$) δ 7.05 (d, J = 8.4 Hz, 2H), 6.68 (d, J = 8.8 Hz, 2H), 4.51 (s, 2H), 3.34–3.39 (m, 4H), 2.25–2.33 (m, 8H), 2.05 (s, 3H), 1.60–1.70 (m, 8H), 1.17–1.31 (m, 14H), 0.88 (t, J = 6.8 Hz, 3H). LC–MS (ESI): *m/z* 439.4 $(M + H)^+$.

N-((3s,5s,7s)-Adamantan-1-yl)-2-(4-chlorophenyl)-N-(4-(diethylamino)benzyl)acetamide (29)—Yield: 79%. ^{1}H NMR (400 MHz, $CDCl_3$) δ 7.28 (d, J = 8.8 Hz, 2H), 7.14 (d, J = 8.4 Hz, 2H), 7.09 (d, J = 8.4 Hz, 2H), 6.71 (d, J = 8.8 Hz, 2H), 4.50 (s, 2H), 3.62 (s, 2H), 3.36–3.41 (m, 4H), 2.27 (s, 6H), 2.06–2.07 (m, 3H), 1.60–1.70 (m, 6H), 1.21 (t, J = 7.2 Hz, 6H). LC–MS (ESI): *m/z* 465.2 $(M + H)^+$.

N-((3s,5s,7s)-Adamantan-1-yl)-N-(4-(diethylamino)benzyl)-2-phenylacetamide (30)—Yield: 70%. ^{1}H NMR (400 MHz, $CDCl_3$) δ 7.29–7.32 (m, 2H), 7.22–7.26 (m, 3H), 7.10 (d, J = 8.4 Hz, 2H), 6.71 (d, J = 8.8 Hz, 2H), 4.50 (s, 2H), 3.67 (s, 2H), 3.36–3.41 (m, 4H), 2.28 (s, 6H), 2.06–2.07 (m, 3H), 1.60–1.70 (m, 6H), 1.21 (t, J = 7.2 Hz, 6H). LC–MS (ESI): *m/z* 431.1 $(M + H)^+$.

N-(4-(Diethylamino)benzyl)-N-heptyl-4-methylbenzenesulfonamide (31)—Yield: 87%. ^{1}H NMR (400 MHz, $CDCl_3$) δ 7.74 (d, *J* = 8.4 Hz, 2H), 7.29–7.33 (m, 2H), 7.09 (d, *J* = 8.8 Hz, 2H), 6.61 (d, *J* = 8.4 Hz, 2H), 4.23 (s, 2H), 3.33–3.38 (m, 4H), 3.06–3.09 (m, 2H), 2.46 (s, 3H), 1.17–1.39 (m, 16H), 1.10–1.15 (m, 3H). LC–MS (ESI): *m/z* 430.7 $(M + H)^+$.

N-(4-(Diethylamino)benzyl)-N-heptyl-3-methylbenzenesulfonamide (32)—Yield: 89%. ^{1}H NMR (400 MHz, DMSO-d_6) δ 7.61 (bs, 2H), 7.49–7.50 (m, 2H), 7.06 (d, *J* = 8.4 Hz, 2H), 6.60 (d, *J* = 8.4 Hz, 2H), 4.14 (s, 2H), 3.28–3.33 (m, 4H), 2.96–3.00 (m, 2H), 2.40 (s, 3H), 1.14–1.24 (m, 4H), 1.04–1.08 (m, 12H), 0.81–0.83 (m, 3H). LC–MS (ESI): *m/z* 432.0 $(M + H)^+$.

N-(4-(Diethylamino)benzyl)-N-heptyl-4-isopropylbenzenesulfonamide (33)—Yield: 81%. ^{1}H NMR (400 MHz, $CDCl_3$) δ 7.77 (d, *J* = 8.4 Hz, 2H), 7.37 (d, *J* = 8.0 Hz, 2H), 7.07 (d, *J* = 8.4 Hz, 2H), 6.61 (d, *J* = 8.8 Hz, 2H), 4.24–4.27 (m, 2H), 3.34–3.38 (m, 4H), 2.97–3.32 (m, 3H), 1.10–1.38 (m, 22H), 0.85–0.89 (m, 3H). LC–MS (ESI): *m/z* 460.2 $(M + H)^+$.

N-(4-(Diethylamino)benzyl)-N-heptyl-4-methoxybenzenesulfonamide (34)—Yield: 89%. ^{1}H NMR (400 MHz, $CDCl_3$) δ 7.77–7.80 (m, 2H), 7.08 (d, *J* = 8.4 Hz, 2H), 6.99 (d, *J* = 8.8 Hz, 2H), 6.61 (d, *J* = 8.4 Hz, 2H), 4.22 (s, 2H), 3.90 (s, 3H), 3.33–3.38 (m, 4H), 3.05–3.09 (m, 2H), 1.15–1.40 (m, 16H), 0.83–0.89 (m, 3H). LC–MS (ESI): *m/z* 448.2 $(M + H)^+$.

N-(4-(Diethylamino)benzyl)-N-heptyl-4-isopropoxybenzenesulfonamide (35)—Yield: 61%. ^{1}H NMR (400 MHz, DMSO-d_6) δ 7.76 (d, *J* = 8.08 Hz, 2H), 7.13 (d, *J* = 8.8 Hz, 2H), 7.06 (d, *J* = 8.4 Hz, 2H), 6.60 (d, *J* = 8.0 Hz, 2H), 4.10 (s, 2H), 3.86 (s, 3H), 3.28–3.34 (m, 4H), 2.93–2.96 (m, 2H), 1.03–1.23 (m, 20H), 0.79–0.83 (m, 3H). LC–MS (ESI): *m/z* 475.4 $(M + H)^+$.

N-(4-(Diethylamino)benzyl)-4-fluoro-N-heptylbenzenesulfonamide (36)—Yield: 77%. ^{1}H NMR (400 MHz, $CDCl_3$) δ 7.83–7.87 (m, 2H), 7.16–7.21 (m, 2H), 7.05 (d, *J* = 8.4 Hz, 2H), 6.60 (d, *J* = 8.4 Hz, 2H), 4.25 (s, 2H), 3.33–3.38 (m, 4H), 3.08–3.13 (m, 2H), 1.02–1.40 (m, 16H), 0.88–0.92 (m, 3H). LC–MS (ESI): *m/z* 436.0 $(M + H)^+$.

4-Chloro-N-(4-(diethylamino)benzyl)-N-heptylbenzenesulfonamide (37)—Yield: 83%. ^{1}H NMR (400 MHz, $CDCl_3$) δ 7.77 (d, *J* = 8.4 Hz, 2H), 7.48 (d, *J* = 8.4 Hz, 2H), 7.06 (d, *J* = 8.8 Hz, 2H), 6.60 (d, *J* = 8.4 Hz, 2H), 4.25 (s, 2H), 3.33–3.38 (m, 4H), 3.08–3.12 (m, 2H), 1.04–1.42 (m, 16H), 0.88–0.92 (m, 3H). LC–MS (ESI): *m/z* 450.7 $(M + H)^+$.

N-(4-(Diethylamino)benzyl)-N-heptyl-1-phenylmethanesulfonamide (38)—Yield: 63%. ^{1}H NMR (400 MHz, $CDCl_3$) δ 7.35–7.40 (m, 5H), 7.16 (d, *J* = 8.4 Hz, 2H), 6.65 (d, *J* = 8.4 Hz, 2H), 4.05–4.25 (m, 4H), 3.34–3.39 (m, 4H), 2.93–2.96 (m, 2H), 1.03–1.41 (m, 16H), 0.88–0.92 (m, 3H). LC–MS (ESI): *m/z* 431.2 $(M + H)^+$.

N-(4-(Diethylamino)benzyl)-N-heptylbutane-1-sulfonamide (39)—Yield: 60%. ^{1}H NMR (400 MHz, $CDCl_3$) δ 7.19 (d, *J* = 8.4 Hz, 2H), 6.66 (d, *J* = 8.8 Hz, 2H), 4.31 (s, 2H), 3.40–3.40 (m, 4H), 3.14–3.16 (m, 2H), 2.88–2.92 (m, 2H), 1.77–1.81 (m, 2H), 0.88–1.57 (m, 24H). LC–MS (ESI): *m/z* 398.0 $(M + H)^+$.

N-(4-(Diethylamino)benzyl)-N-heptyl-2-phenylacetamide (40)—Yield: 70%. ^{1}H NMR (400 MHz, DMSO-d_6) δ 7.25–7.33 (m, 5H), 7.08 (d, *J* = 8.4 Hz, 1H), 6.94 (d, *J* = 8.8 Hz, 1H), 6.65–6.69 (m, 2H), 4.47–4.51 (m, 2H), 3.81–3.82 (m, 2H), 3,31–3.40 (m, 5H),

3.24–3.28 (m, 1H), 1.12–1.29 (m, 16H), 0.88–0.92 (m, 3H). LC–MS (ESI): *m/z* 396.1 (M + H)$^+$.

2-(4-Chlorophenyl)-N-(4-(diethylamino)benzyl)-N-heptylacetamide (41)—Yield: 65%. ^{1}H NMR (400 MHz, DMSO-d_6) δ 7.16–7.35 (m, 4H), 7.17 (d, *J* = 8.4 Hz, 1H), 7.08 (d, *J* = 6.4 Hz, 1H), 6.66–6.71 (m, 2H), 4.51 (s, 2H), 3.80–3.81 (m, 2H), 3,35–3.39 (m, 5H), 3.26–3.28 (m, 1H), 1.14–1.67 (m, 16H), 0.89–0.92 (m, 3H). LC–MS (ESI): *m/z* 428.8 (M + H)$^+$.

N-(4-(Diethylamino)benzyl)-4-(dimethylamino)-N-heptylbenzamide (42)—Yield: 80%. ^{1}H NMR (400 MHz, $CDCl_3$) δ 7.37 (d, *J* = 8.4 Hz, 2H), 7.09 (bs, 2H), 6.64–6.66 (m, 4H), 4.55 (s, 2H), 3.32–3.37 (m, 6H), 2.98 (s, 6H), 1.57–1.61 (m, 2H), 1.14–1.28 (m, 14H), 0.86 (t, *J* = 7.2 Hz, 6H). LC–MS (ESI): *m/z* 424.4 (M + H)$^+$.

N-(4-(Diethylamino)benzyl)-N-heptylcyclohexanecarboxamide (43)—Yield: 91%. ^{1}H NMR (400 MHz, $CDCl_3$) δ 6.97–7.06 (m, 4H), 6.59–6.66 (m, 4H), 4.11–4.46 (m, 2H), 3.14–3.37 (m, 6H), 2.47–2.51 (m, 1H), 1.51–1.82 (m, 10H), 1.01–1.49 (m, 16H), 0.84–0.90 (m, 3H). LC–MS (ESI): *m/z* 387.1 (M + H)$^+$.

N-(4-(Diethylamino)benzyl)-N-heptyloctanamide (44)—Yield: 95%. ^{1}H NMR (400 MHz, MeOD) δ 7.02–7.09 (m, 2H), 6.67–6.87 (m, 2H), 4.49 (s, 2H), 3.24–3.41 (m, 6H), 2.43 (t, *J* = 7.2 Hz, 2H), 1.13–1.68 (m, 26H), 0.89–0.95 (m, 3H). LC–MS (ESI): *m/z* 402.9 (M + H)$^+$.

N-(4-Chlorophenyl)-N-(4-(diethylamino)benzyl)benzenesulfonamide (45)—Yield: 73%. ^{1}H NMR (400 MHz, DMSO-d_6) δ 7.64–7.73 (m, 5H), 7.32–7.34 (m, 2H), 6.96–7.05 (m, 4H), 6.50 (d, *J* = 7.2 Hz, 2H), 4.63 (s, 2H), 3.23–3.26 (m, 4H), 1.02–1.04 (m, 6H). LC–MS (ESI): *m/z* 428.9 (M + H)$^+$.

N-(4-Chlorophenyl)-N-(4-(diethylamino)benzyl)-4-fluorobenzenesulfonamide (46)—Yield: 69%. ^{1}H NMR (400 MHz, DMSO-d_6) δ 7.68–7.70 (m, 2H), 7.44–7.49 (m, 2H), 7.33 (d, *J* = 8.8 Hz, 2H), 7.06 (d, *J* = 8.4 Hz, 2H), 6.96 (d, *J* = 8.8 Hz, 2H), 6.50 (d, *J* = 8.8 Hz, 2H), 4.62 (s, 2H), 3.22–3.28 (m, 4H), 1.02 (t, *J* = 6.8 Hz, 6H). LC–MS (ESI): *m/z* 446.9 (M + H)$^+$.

4-Chloro-N-(4-chlorophenyl)-N-(4-(diethylamino)benzyl)benzenesulfonamide (47)—Yield: 65%. ^{1}H NMR (400 MHz, DMSO-d_6) δ 7.70 (d, *J* = 8.8 Hz, 2H), 7.63 (d, *J* = 8.8 Hz, 2H), 7.34 (d, *J* = 8.8 Hz, 2H), 7.07 (d, *J* = 8.8 Hz, 2H), 6.96 (d, *J* = 8.8 Hz, 2H), 6.50 (d, *J* = 8.8 Hz, 2H), 4.62 (s, 2H), 3.22–3.28 (m, 4H), 1.01–1.06 (m, 6H). LC–MS (ESI): *m/z* 463.0 (M + H)$^+$.

N-(4-Chlorophenyl)-N-(4-(diethylamino)benzyl)-4-methoxybenzenesulfonamide (48)—Yield: 55%. ^{1}H NMR (400 MHz, DMSO-d_6) δ 7.56 (d, *J* = 8.8 Hz, 2H), 7.32 (d, *J* = 8.8 Hz, 2H), 7.13 (d, *J* = 8.8 Hz, 2H), 7.05 (d, *J* = 8.8 Hz, 2H), 6.96 (d, *J* = 8.8 Hz, 2H), 6.50 (d, *J* = 8.8 Hz, 2H), 4.58 (s, 2H), 3.86 (s, 3H), 3.22–3.27 (m, 4H), 1.02 (t, *J* = 6.8 Hz, 6H). LC–MS (ESI): *m/z* 459.1 (M + H)$^+$.

N-(4-Chlorophenyl)-N-(4-(diethylamino)benzyl)-4-methylbenzenesulfonamide (49)—Yield: 79%. ^{1}H NMR (400 MHz, DMSO-d_6) δ 7.31–7.51 (m, 6H), 7.03–7.05 (m, 2H), 6.96 (d, *J* = 8.8 Hz, 2H), 6.49 (d, *J* = 8.8 Hz, 2H), 4.59 (s, 2H), 3.22–3.27 (m, 4H), 2,42 (s, 3H), 1.02 (t, *J* = 6.8 Hz, 6H). LC–MS (ESI): *m/z* 443.2 (M + H)$^+$.

N-(4-Chlorophenyl)-N-(4-(diethylamino)benzyl)-3-methylbenzenesulfonamide (50)—Yield: 65%. ^{1}H NMR (400 MHz, DMSO-d_6) δ 7.38–7.53 (m, 4H), 7.32 (d, J = 8.4 Hz, 2H), 7.04 (d, J = 8.8 Hz, 2H), 6.96 (d, J = 8.8 Hz, 2H), 6.50 (d, J = 8.8 Hz, 2H), 4.61 (s, 2H), 3.22–3.28 (m, 4H), 2,40 (s, 3H), 1.02 (t, J = 6.8 Hz, 6H). LC–MS (ESI): *m/z* 443.0 $(M + H)^+$.

N-(4-Chlorophenyl)-N-(4-(diethylamino)benzyl)-4-isopropylbenzenesulfonamide (51)—Yield: 89%. ^{1}H NMR (400 MHz, DMSO-d_6) δ 7.56 (d, J = 8.4 Hz, 2H), 7.49 (d, J = 8.0 Hz, 2H), 7.32 (d, J = 8.8 Hz, 2H), 7.06 (d, J = 8.8 Hz, 2H), 6.96 (d, J = 8.8 Hz, 2H), 6.50 (d, J = 8.8 Hz, 2H), 4.61 (s, 2H), 3.23–3.26 (m, 4H), 2.98–3.05 (m, 1H), 1.25 (d, J = 6.8 Hz, 6H), 1.03 (t, J = 6.4 Hz, 6H). LC–MS (ESI): *m/z* 471.1 $(M + H)^+$.

N,2-bis(4-Chlorophenyl)-N-(4-(diethylamino)benzyl)acetamide (52)—Yield: 79%. ^{1}H NMR (400 MHz, DMSO-d_6) δ 7.44 (d, J = 8.4 Hz, 2H), 7.32 (d, J = 8.4 Hz, 2H), 7.09–7.14 (m, 4H), 6.91 (d, J = 8.8 Hz, 2H), 6.54 (d, J = 8.8 Hz, 2H), 4.71 (s, 2H), 3.42 (s, 2H), 3.25–3.31 (m, 4H), 1.05 (t, J = 6.4 Hz, 6H). LC–MS (ESI): *m/z* 442.8 $(M + H)^+$.

N-(4-Chlorophenyl)-N-(4-(diethylamino)benzyl)cyclohexanecarboxamide (53)—Yield: 68%. ^{1}H NMR (400 MHz, DMSO-d_6) δ 7.44 (d, J = 8.4 Hz, 2H), 7.11 (d, J = 8.4 Hz, 2H), 6.89 (d, J = 8.4 Hz, 2H), 6.55 (d, J = 8.4 Hz, 2H), 4.65 (s, 2H), 3.26–3.31 (m, 4H), 2.08 (bs, 1H), 1.36–1.63 (m, 7H), 0.93–1.13 (m, 9H). LC–MS (ESI): *m/z* 399.4 $(M + H)^+$.

N-(4-(Diethylamino)benzyl)-N-(p-tolyl)benzenesulfonamide (54)—Yield: 80%. ^{1}H NMR (400 MHz, DMSO-d_6) δ 7.60–7.72 (m, 5H), 7.04 (d, J = 8.0 Hz, 2H), 6.96 (d, J = 8.8 Hz, 2H), 6.87 (d, J = 8.4 Hz, 2H), 6.50 (d, J = 8.8 Hz, 2H), 4.60 (s, 2H), 3.23–3.28 (m, 4H), 2.23 (s, 3H), 1.03 (t, J = 7.2 Hz, 6H). LC–MS (ESI): *m/z* 408.9 $(M + H)^+$.

N-(4-(Diethylamino)benzyl)-4-fluoro-N-(p-tolyl)benzenesulfonamide (55)—Yield: 83%. ^{1}H NMR (400 MHz, DMSO-d_6) δ 7.66–7.68 (m, 2H), 7.43–7.47 (m, 2H), 7.06 (d, J = 8.0 Hz, 2H), 6.96 (d, J = 8.8 Hz, 2H), 6.89 (d, J = 8.4 Hz, 2H), 6.50 (d, J = 8.8 Hz, 2H), 4.60 (s, 2H), 3.22–3.30 (m, 4H), 2.23 (s, 3H), 1.02 (t, J = 7.2 Hz, 6H). LC–MS (ESI): *m/z* 427.2 $(M + H)^+$.

4-Chloro-N-(4-(diethylamino)benzyl)-N-(p-tolyl)benzenesulfonamide (56)—Yield: 85%. ^{1}H NMR (400 MHz, DMSO-d_6) δ 7.67–7.70 (m, 2H), 7.61–7.63 (m, 2H), 7.06 (d, J = 8.0 Hz, 2H), 6.96 (d, J = 8.8 Hz, 2H), 6.90 (d, J = 8.4 Hz, 2H), 6.50 (d, J = 8.8 Hz, 2H), 4.60 (s, 2H), 3.22–3.28 (m, 4H), 2.23 (s, 3H), 1.02 (t, J = 7.2 Hz, 6H). LC–MS (ESI): *m/z* 442.8 $(M + H)^+$.

N-(4-(Diethylamino)benzyl)-4-methoxy-N-(p-tolyl)benzenesulfonamide (57)—Yield: 91%. ^{1}H NMR (400 MHz, DMSO-d_6) δ 7.53–7.56 (m, 2H), 7.11–7.13 (m, 2H), 7.04 (d, J = 8.4 Hz, 2H), 6.96 (d, J = 8.4 Hz, 2H), 6.88 (d, J = 8.4 Hz, 2H), 6.49 (d, J = 8.8 Hz, 2H), 4.56 (s, 2H), 3.86 (s, 3H), 3.22–3.27 (m, 4H), 2.23 (s, 3H), 1.02 (t, J = 7.2 Hz, 6H). LC–MS (ESI): *m/z* 439.1 $(M + H)^+$.

N-(4-(Diethylamino)benzyl)-4-methyl-N-(p-tolyl)benzenesulfonamide (58)—Yield: 94%. ^{1}H NMR (400 MHz, DMSO-d_6) δ 7.50 (d, J = 8.0 Hz, 2H), 7.40 (d, J = 8.4 Hz, 2H), 7.04 (d, J = 8.0 Hz, 2H), 6.96 (d, J = 8.8 Hz, 2H), 6.87 (d, J = 8.4 Hz, 2H), 6.49 (d, J = 8.8 Hz, 2H), 4.57 (s, 2H), 3.22–3.27 (m, 4H), 2.42 (s, 3H), 2.22 (s, 3H), 1.02 (t, J = 7.2 Hz, 6H). LC–MS (ESI): *m/z* 423.0 $(M + H)^+$.

N-(4-(Diethylamino)benzyl)-3-methyl-N-(p-tolyl)benzenesulfonamide (59)— Yield: 72%. ^{1}H NMR (400 MHz, DMSO-d_6) δ 7.37–7.51 (m, 4H), 7.05 (d, J = 8.4 Hz, 2H), 6.96 (d, J = 8.4 Hz, 2H), 6.86–6.88 (m, 2H), 6.50 (d, J = 8.8 Hz, 2H), 4.59 (s, 2H), 3.22–3.28 (m, 4H), 2.39 (s, 3H), 2.23 (s, 3H), 1.03 (t, J = 7.2 Hz, 6H). LC–MS (ESI): *m/z* 423.4 $(M + H)^+$.

N-(4-(Diethylamino)benzyl)-4-isopropyl-N-(p-tolyl)benzenesulfonamide (60)— Yield: 86%. ^{1}H NMR (400 MHz, DMSO-d_6) δ 7.54–7.56 (m, 2H), 7.47 (d, J = 8.4 Hz, 2H), 7.05 (d, J = 8.0 Hz, 2H), 6.96 (d, J = 8.4 Hz, 2H), 6.89 (d, J = 8.4 Hz, 2H), 6.49 (d, J = 8.8 Hz, 2H), 4.58 (s, 2H), 3.22–3.28 (m, 4H), 2.98–3.05 (m, 1H), 2.23 (s, 3H), 1.25 (d, J = 7.2 Hz, 6H), 1.02 (t, J = 7.2 Hz, 6H). LC–MS (ESI): *m/z* 450.9 $(M + H)^+$.

N-(4-(Diethylamino)benzyl)-2-phenyl-N-(p-tolyl)acetamide (61)—Yield: 86%. ^{1}H NMR (400 MHz, DMSO-d_6) δ 7.17–7.27 (m, 5H), 7.05 (d, J = 7.2 Hz, 2H), 6.97 (d, J = 8.0 Hz, 2H), 6.91 (d, J = 8.8 Hz, 2H), 6.54 (d, J = 8.8 Hz, 2H), 4.69 (s, 2H), 3.35–3.40 (m, 2H), 3.25–3.31 (m, 4H), 2.30 (s, 3H), 1.05 (t, J = 7.2 Hz, 6H). LC–MS (ESI): *m/z* 387.5 $(M + H)^+$.

2-(4-Chlorophenyl)-N-(4-(diethylamino)benzyl)-N-(p-tolyl)acetamide (62)— Yield: 86%. ^{1}H NMR (400 MHz, DMSO-d_6) δ 7.31 (d, J = 8.4 Hz, 2H), 7.18 (d, J = 8.0 Hz, 2H), 7.08 (d, J = 8.0 Hz, 2H), 6.98 (d, J = 8.0 Hz, 2H), 6.91 (d, J = 8.4 Hz, 2H), 6.54 (d, J = 8.8 Hz, 2H), 4.68 (s, 2H), 3.35–3.38 (m, 2H), 3.25–3.32 (m, 4H), 2.30 (s, 3H), 1.05 (t, J = 7.2 Hz, 6H). LC–MS (ESI): *m/z* 420.7 $(M + H)^+$.

N-(4-(Diethylamino)benzyl)-N-(p-tolyl)cyclohexanecarboxamide (63)—Yield: 84%. ^{1}H NMR (400 MHz, DMSO-d_6) δ 7.18 (d, J = 8.0 Hz, 2H), 6.94 (d, J = 8.0 Hz, 2H), 6.89 (d, J = 8.4 Hz, 2H), 6.54 (d, J = 8.4 Hz, 2H), 4.63 (s, 2H), 3.26–3.31 (m, 4H), 2.30 (s, 3H), 2.08–2.14 (m, 1H), 1.35–1.62 (m, 8H), 0.86–1.09 (m, 8H). LC–MS (ESI): *m/z* 379.5 $(M + H)^+$.

Radioligand Competition Binding Assays

CB ligand competition binding assay was carried out as described previously.[33, 41] Briefly, non-radioactive ligands were diluted in binding buffer, supplemented with 10% dimethyl sulfoxide and 0.4% methyl cellulose. Each assay plate well contained a total of 200 μL of reaction mixture comprised of 5 μg of CB_1 (or CB_2) membrane protein, labeled [^{3}H]CP-55,940 ligand at a final concentration of 3 nM and the unlabeled ligand at its varying dilutions as stated above. Plates were incubated at 30 °C for 1 h with gentle shaking. The reaction was terminated by rapid filtration through Unifilter GF/B filter plates using a Unifilter Cell Harvester (PerkinElmer). After the plate was allowed to dry overnight, 30 μL MicroScint-0 cocktail (PerkinElmer) was added to each well and the radioactivity was counted by using a PerkinElmer TopCounter. All assays were performed in duplicate and data points represented as mean ± S.E.M. Bound radioactivity data was analyzed for K_i values using non-linear regression analysis via GraphPad Prism 5.0 software.

The saturation binding of [^{3}H]CP-55,940 to the membrane proteins was performed as described previously.[33, 34] Briefly, the CB_1 (or CB_2) membrane fractions (5 μg) were incubated with increasing concentrations of [^{3}H]CP-55,940 (0.05–4 nM) in 96-well plates at 30 °C with slow shaking for 1 h. The incubation buffer was composed of 50 mM Tris-HCl (pH 7.4), 5 mM $MgCl_2$, 2.5 mM EGTA and 0.1% (w/v) fatty acid free BSA. Ligand was diluted in incubation buffer supplemented with 10% dimethyl sulfoxide and 0.4% methyl cellulose. Non-specific binding was determined in the presence of unlabeled CP-55,940 (5,000 nM). The reaction was terminated and the radioactivity was counted as stated above.

Non-linear regression analysis revealed the receptor density (B_{max}) and the equilibrium dissociation constant (K_d) values of [^{3}H]CP-55,940 for the CB_2 receptor.

cAMP Assays

Cellular cAMP levels were measured according to reported method with modifications using LANCE cAMP 384 kits (PerkinElmer).[33, 34] The assay is based on competition between a Europium-labeled cAMP trace complex and total cAMP for binding sites on cAMP-specific antibodies labeled with a fluorescent dye. CB_2 receptor wild type (WT) transfected CHO cells were seeded in a 384-well white ProxiPlates with a density of 2000 cells per well in 5 μL of RPMI-1640 medium containing 1% dialysed FBS, 25 mM HEPES, 100 μg/mL pennicilin, 100 U/ml strepmicin and 200 μg/mL of G-418. After culture overnight, 2.5 μL of cAMP antibody and RO20-1724 (final consentration50 μM) in stimulation buffer (DPBS 1×, containing 0.1% BSA) was added to each well, followed by addition of either 2.5 μL compound or forskolin (final 5 μM) for agonist-inhibited adenylate cyclase (AC) activity assay. After incubated at room temperature for 45 min, 10 μL of detection reagent was added into each well. The plate was then incubated for 1 h at room temperature and measured in Synergy H1 hybrid reader (BioTek) with excitation at 340 nm and emission at 665 nm. Each cAMP determination was made via at least two independent experiments, each in triplicate. EC_{50} values were determined by nonlinear regression, dose–response curves (GraphPad Prism 5).

In Vitro Osteoclast Formation Assay

RAW 264.7 cells were seeded at 3×10^3 cells per well using 96-well multiplates and cultured for 24 h in αMEM with 10% fetal bovine serum (FBS). Thereafter, the cell medium was changed with same medium containing RANKL (15 ng/mL) and various concentrations of tested compounds. After 5 days, cells were fixed and stained for tartrate-resistant acid phosphate (TRAP) (Sigma) activity according to the recommendation of the manufacturer. $TRAP^+$ multinucleated cells with more than three nuclei were counted as osteoclasts.[42, 43]

Cytotoxicity Assay of Top Compounds on Precursor Osteoclasts

To study whether the inhibitory effects of our compounds on osteoclast development are due to their direct cytotoxicity on RAW 264.7 cells, we performed cell proliferation assay. RAW 264.7 cells (3×10^3 cells) were plated on 96-well plates and treated with the indicated concentrations of top compounds and then incubated for 3 days. The percentage of cell survival was determined with the MTT assay as described before.[33, 44]

3D QSAR CoMFA Studies

Out of 46 compounds from Tables 1–4, 44 compounds were used in the CoMFA QSAR studies. 2 compounds showed no binding were ignored in the analysis. Approximately 75% (33 compounds) and 25% (11 compounds) were randomly selected as a training set and test set, respectively. SYBYL-X 1.3 was used for the QSAR studies and analysis. Using our established protocol, molecular dynamic simulations were carried out for our best compound **57**. Briefly, dynamic simulations were simulated at 300 K with a time steps of 1 fs for a total duration of 300 ps, and conformation samples were collected at every 1 ps, resulting in 300 conformers of compound **57**.

All conformers were then minimized and converged into five families. Then we compared these five representative conformers with the docking pose from the molecular docking experiment using our in-house 3D CB_2 receptor model. The docking experiment was done using the Surflex-Dock module from the Tripos modeling software. The conformer with maximum agreement between these two experiments was chosen as a preferred conformer

for further CoMFA studies. All structures were built and energy minimized under the Tripos force field with 0.05 kcal/(mol A°). Gasteiger-Huckel method was used to calculate the charges. Energy minimization was performed by Powell method with 2000 iterations. Structural alignments of all molecules in the training and test sets to the preferred conformer of compound **57** were performed using the MultiFit program in Sybyl-X1.3. The CoMFA study was then carried out using the SYBYL/CoMFA module. Leave one-out cross-validation (LOOCV) partial least squares (PLS) analysis was then performed with a minimum σ (column filter) value of 5.0 kcal·mol^{-1} to improve the signal-to-noise ratio by omitting those lattice points whose energy variation was below this threshold. The final model (non-cross-validated analysis) was developed from the LOOCV model with the highest cross-validated r^2, using the optimal number of components determined by the LOOCV model.

Acknowledgments

The authors from the University of Pittsburgh gratefully acknowledge the financial support for our laboratory from the NIH R01DA025612 and R21HL109654 and P50 GM067082. Authors would also like to acknowledge the collaboration support from the National Natural Science Foundation of China (NSFC81090410, NSFC90913018).

ABBREVIATIONS

CB	cannabinoid
GALAHAD	genetic algorithm-based pharmacophore alignment
HB	H-bond
SAR	structure-activity relationship
OCL	osteoclast
QSAR	quantitative structure–activity relationship
CoMFA	comparative molecular field analysis
MD	molecular dynamic
MM	molecular mechanics
LOOCV	leave-one-out cross-validation
PLS	partial least squares
SEE	standard error of estimate
MTA	material transfer agreement
TLC	thin-layer chromatography
EA	ethyl acetate
DCM	dichloromethane
EGTA	ethylene glycol tetraacetic acid
BSA	bovine serum albumin
WT	wild type
DPBS	dulbecco's phosphate-buffered saline
AC	adenylate cyclase
RANKL	receptor activator of nuclear factor kappa-B ligand

TRAP tartrate-resistant acid phosphate

REFERENCES

1. Devane WA, Hanus L, Breuer A, Pertwee RG, Stevenson LA, Griffin G, Gibson D, Mandelbaum A, Etinger A, Mechoulam R. Isolation and structure of a brain constituent that binds to the cannabinoid receptor. Science. 1992; 258:1946–1949. [PubMed: 1470919]
2. Mechoulam R, Ben-Shabat S, Hanus L, Ligumsky M, Kaminski NE, Schatz AR, Gopher A, Almog S, Martin BR, Compton DR, et al. Identification of an endogenous 2-monoglyceride, present in canine gut, that binds to cannabinoid receptors. Biochem. Pharmacol. 1995; 50:83–90. [PubMed: 7605349]
3. Sugiura T, Kondo S, Sukagawa A, Nakane S, Shinoda A, Itoh K, Yamashita A, Waku K. 2-Arachidonoylglycerol: a possible endogenous cannabinoid receptor ligand in brain. Biochem. Biophys. Res. Commun. 1995; 215:89–97. [PubMed: 7575630]
4. Bayewitch M, Rhee MH, Avidor-Reiss T, Breuer A, Mechoulam R, Vogel Z. (−)-Delta9-tetrahydrocannabinol antagonizes the peripheral cannabinoid receptor-mediated inhibition of adenylyl cyclase. J. Biol. Chem. 1996; 271:9902–9905. [PubMed: 8626625]
5. Felder CC, Joyce KE, Briley EM, Mansouri J, Mackie K, Blond O, Lai Y, Ma AL, Mitchell RL. Comparison of the pharmacology and signal transduction of the human cannabinoid CB1 and CB2 receptors. Mol. Pharmacol. 1995; 48:443–450. [PubMed: 7565624]
6. Matsuda LA, Lolait SJ, Brownstein MJ, Young AC, Bonner TI. Structure of a cannabinoid receptor and functional expression of the cloned cDNA. Nature. 1990; 346:561–564. [PubMed: 2165569]
7. Munro S, Thomas KL, Abu-Shaar M. Molecular characterization of a peripheral receptor for cannabinoids. Nature. 1993; 365:61–65. [PubMed: 7689702]
8. Hohmann AG. Spinal and peripheral mechanisms of cannabinoid antinociception: behavioral, neurophysiological and neuroanatomical perspectives. Chem. Phys. Lipids. 2002; 121:173–190. [PubMed: 12505699]
9. Karsak M, Gaffal E, Date R, Wang-Eckhardt L, Rehnelt J, Petrosino S, Starowicz K, Steuder R, Schlicker E, Cravatt B, Mechoulam R, Buettner R, Werner S, Di Marzo V, Tuting T, Zimmer A. Attenuation of allergic contact dermatitis through the endocannabinoid system. Science. 2007; 316:1494–1497. [PubMed: 17556587]
10. Palazuelos J, Davoust N, Julien B, Hatterer E, Aguado T, Mechoulam R, Benito C, Romero J, Silva A, Guzman M, Nataf S, Galve-Roperh I. The CB2 cannabinoid receptor controls myeloid progenitor trafficking. J. Biol. Chem. 2008; 283:13320–13329. [PubMed: 18334483]
11. Guindon J, Hohmann AG. The endocannabinoid system and cancer: therapeutic implication. Brit. J. Pharmacol. 2011; 163:1447–1463. [PubMed: 21410463]
12. Oesch S, Gertsch J. Cannabinoid receptor ligands as potential anticancer agents--high hopes for new therapies? J. Pharm. Pharmacol. 2009; 61:839–853. [PubMed: 19589225]
13. Idris AI, Ralston SH. Cannabinoids and Bone: Friend or Foe? Calcified Tissue Int. 2010; 87:285–297.
14. Hillard CJ. Role of cannabinoids and endocannabinoids in cerebral ischemia. Curr. Pharm. Des. 2008; 14:2347–2361. [PubMed: 18781985]
15. Hegde VL, Hegde S, Cravatt BF, Hofseth LJ, Nagarkatti M, Nagarkatti PS. Attenuation of experimental autoimmune hepatitis by exogenous and endogenous cannabinoids: involvement of regulatory T cells. Mol. Pharmacol. 2008; 74:20–33. [PubMed: 18388242]
16. Munoz-Luque J, Ros J, Fernandez-Varo G, Tugues S, Morales-Ruiz M, Alvarez CE, Friedman SL, Arroyo V, Jimenez W. Regression of fibrosis after chronic stimulation of cannabinoid CB2 receptor in cirrhotic rats. J. Pharmacol. Exp. Ther. 2008; 324:475–483. [PubMed: 18029545]
17. Izzo AA, Camilleri M. Emerging role of cannabinoids in gastrointestinal and liver diseases: basic and clinical aspects. Gut. 2008; 57:1140–1155. [PubMed: 18397936]
18. Pacher P, Batkai S, Kunos G. The endocannabinoid system as an emerging target of pharmacotherapy. Pharmacol. Rev. 2006; 58:389–462. [PubMed: 16968947]

19. Compton DR, Rice KC, De Costa BR, Razdan RK, Melvin LS, Johnson MR, Martin BR. Cannabinoid structure-activity relationships: correlation of receptor binding and in vivo activities. J. Pharmacol. Exp. Ther. 1993; 265:218–226. [PubMed: 8474008]
20. Huffman JW. Cannabimimetic indoles, pyrroles and indenes. Curr. Med. Chem. 1999; 6:705–720. [PubMed: 10469887]
21. Palmer SL, Thakur GA, Makriyannis A. Cannabinergic ligands. Chem. Phys. Lipids. 2002; 121:3–19. [PubMed: 12505686]
22. Raitio KH, Salo OM, Nevalainen T, Poso A, Jarvinen T. Targeting the cannabinoid CB2 receptor: mutations, modeling and development of CB2 selective ligands. Curr. Med. Chem. 2005; 12:1217–1237. [PubMed: 15892633]
23. Marriott KS, Huffman JW. Recent advances in the development of selective ligands for the cannabinoid CB(2) receptor. Curr. Top. Med. Chem. 2008; 8:187–204. [PubMed: 18289088]
24. Yang P, Wang L, Xie XQ. Latest advances in novel cannabinoid CB(2) ligands for drug abuse and their therapeutic potential. Future Med. Chem. 2012; 4:187–204. [PubMed: 22300098]
25. Rinaldi-Carmona M, Barth F, Millan J, Derocq JM, Casellas P, Congy C, Oustric D, Sarran M, Bouaboula M, Calandra B, Portier M, Shire D, Breliere JC, Le Fur GL. SR 144528, the first potent and selective antagonist of the CB2 cannabinoid receptor. J. Pharmacol. Exp. Ther. 1998; 284:644–650. [PubMed: 9454810]
26. Ross RA, Brockie HC, Stevenson LA, Murphy VL, Templeton F, Makriyannis A, Pertwee RG. Agonist-inverse agonist characterization at CB1 and CB2 cannabinoid receptors of L759633, L759656, and AM630. Br. J. Pharmacol. 1999; 126:665–672. [PubMed: 10188977]
27. Huffman JW, Zengin G, Wu MJ, Lu J, Hynd G, Bushell K, Thompson AL, Bushell S, Tartal C, Hurst DP, Reggio PH, Selley DE, Cassidy MP, Wiley JL, Martin BR. Structure-activity relationships for 1-alkyl-3-(1-naphthoyl)indoles at the cannabinoid CB(1) and CB(2) receptors: steric and electronic effects of naphthoyl substituents. New highly selective CB(2) receptor agonists. Bioorg. Med. Chem. 2005; 13:89–112. [PubMed: 15582455]
28. Kimball ES, Schneider CR, Wallace NH, Hornby PJ. Agonists of cannabinoid receptor 1 and 2 inhibit experimental colitis induced by oil of mustard and by dextran sulfate sodium. Am. J. Physiol. Gastrointest. Liver Physiol. 2006; 291:G364–G371. [PubMed: 16574988]
29. Xi Z-X, Peng X-Q, Li X, Song R, Zhang H-Y, Liu Q-R, Yang H-J, Bi G-H, Li J, Gardner EL. Brain cannabinoid CB2 receptors modulate cocaine's actions in mice. Nat. Neurosci. 2011; 14:1160–1166. [PubMed: 21785434]
30. Lunn CA, Fine JS, Rojas-Triana A, Jackson JV, Fan X, Kung TT, Gonsiorek W, Schwarz MA, Lavey B, Kozlowski JA, Narula SK, Lundell DJ, Hipkin RW, Bober LA. A novel cannabinoid peripheral cannabinoid receptor-selective inverse agonist blocks leukocyte recruitment in vivo. J. Pharmacol. Exp. Ther. 2006; 316:780–788. [PubMed: 16258021]
31. Iwamura H, Suzuki H, Ueda Y, Kaya T, Inaba T. In vitro and in vivo pharmacological characterization of JTE-907, a novel selective ligand for cannabinoid CB2 receptor. J. Pharmacol. Exp. Ther. 2001; 296:420–425. [PubMed: 11160626]
32. Francisco ME, Seltzman HH, Gilliam AF, Mitchell RA, Rider SL, Pertwee RG, Stevenson LA, Thomas BF. Synthesis and structure-activity relationships of amide and hydrazide analogues of the cannabinoid CB(1) receptor antagonist N-(piperidinyl)- 5-(4-chlorophenyl)-1-(2,4-dichlorophenyl)-4-methyl-1H-pyrazole-3-carboxamide (SR141716). J. Med. Chem. 2002; 45:2708–2719. [PubMed: 12061874]
33. Yang P, Myint KZ, Tong Q, Feng R, Cao H, Almehizia AA, Hamed AM, Wang L, Bartlow P, Gao Y, Gertsch J, Teramachi J, Kurihara N, Roodman GD, Cheng T, Xie XQ. Lead Discovery, Chemistry Optimization and Biological Evaluation Studies of Novel Bi-amide Derivatives as CB2 Receptor Inverse Agonists and Osteoclast Inhibitors. J. Med. Chem. 2012; 55:9973–9987. [PubMed: 23072339]
34. Zhang Y, Xie Z, Wang L, Schreiter B, Lazo JS, Gertsch J, Xie XQ. Mutagenesis and computer modeling studies of a GPCR conserved residue W5.43(194) in ligand recognition and signal transduction for CB2 receptor. Int. Immunopharmacol. 2011; 11:1303–1310. [PubMed: 21539938]
35. Bab I, Zimmer A, Melamed E. Cannabinoids and the skeleton: from marijuana to reversal of bone loss. Ann. Med. 2009; 41:560–567. [PubMed: 19634029]

36. Anandarajah AP, Schwarz EM, Totterman S, Monu J, Feng CY, Shao T, Haas-Smith SA, Ritchlin CT. The effect of etanercept on osteoclast precursor frequency and enhancing bone marrow oedema in patients with psoriatic arthritis. Ann. Rheum. Dis. 2008; 67:296–301. [PubMed: 17967829]

37. Myint KZ, Xie XQ. Recent advances in fragment-based QSAR and multidimensional QSAR methods. Int. J. Mol. Sci. 2010; 11:3846–3866. [PubMed: 21152304]

38. Chen JZ, Han XW, Liu Q, Makriyannis A, Wang J, Xie XQ. 3D-QSAR studies of arylpyrazole antagonists of cannabinoid receptor subtypes CB1 and CB2. A combined NMR and CoMFA approach. J. Med. Chem. 2006; 49:625–636. [PubMed: 16420048]

39. Xie XQ, Melvin LS, Makriyannis A. The conformational properties of the highly selective cannabinoid receptor ligand CP-55,940. J. Biol. Chem. 1996; 271:10640–10647. [PubMed: 8631869]

40. Xie XQ, Chen JZ, Billings EM. 3D structural model of the G-protein-coupled cannabinoid CB2 receptor. Proteins. 2003; 53:307–319. [PubMed: 14517981]

41. Gertsch J, Leonti M, Raduner S, Racz I, Chen JZ, Xie XQ, Altmann KH, Karsak M, Zimmer A. Beta-caryophyllene is a dietary cannabinoid. Proc. Natl. Acad. Sci. U. S. A. 2008; 105:9099–9104. [PubMed: 18574142]

42. Feng R, Anderson G, Xiao G, Elliott G, Leoni L, Mapara MY, Roodman GD, Lentzsch S. SDX-308, a nonsteroidal anti-inflammatory agent, inhibits NF-kappaB activity, resulting in strong inhibition of osteoclast formation/activity and multiple myeloma cell growth. Blood. 2007; 109:2130–2138. [PubMed: 17095620]

43. Xu J, Li Z, Luo J, Yang F, Liu T, Liu M, Qiu WW, Tang J. Synthesis and biological evaluation of heterocyclic ring-fused betulinic acid derivatives as novel inhibitors of osteoclast differentiation and bone resorption. J. Med. Chem. 2012; 55:3122–3134. [PubMed: 22435650]

44. Feng R, Ma H, Hassig CA, Payne JE, Smith ND, Mapara MY, Hager JH, Lentzsch S. KD5170, a novel mercaptoketone-based histone deacetylase inhibitor, exerts antimyeloma effects by DNA damage and mitochondrial signaling. Mol. Cancer. Ther. 2008; 7:1494–1505. [PubMed: 18566220]

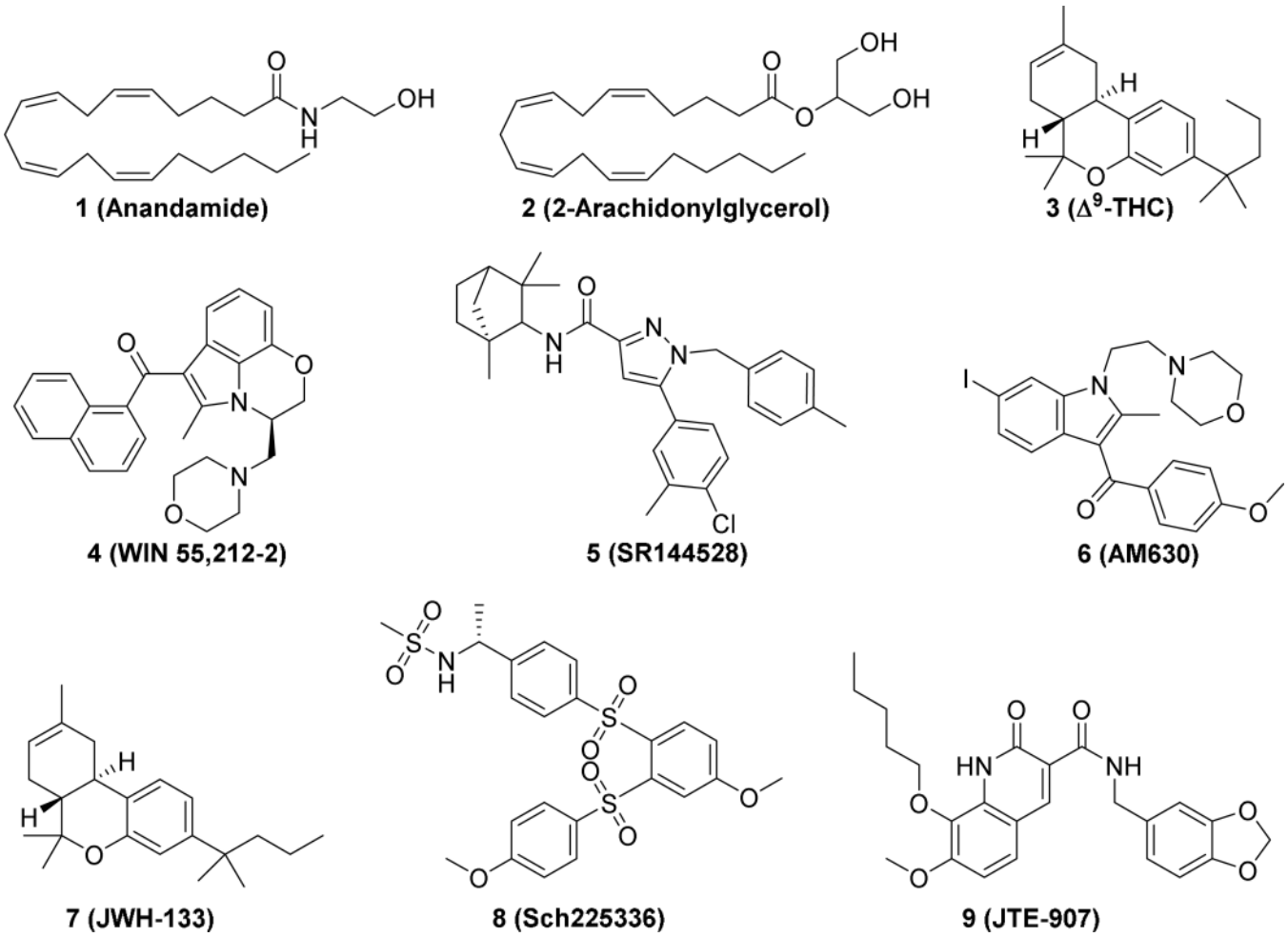

Figure 1.
Representative cannabinoids with various chemical scaffolds.

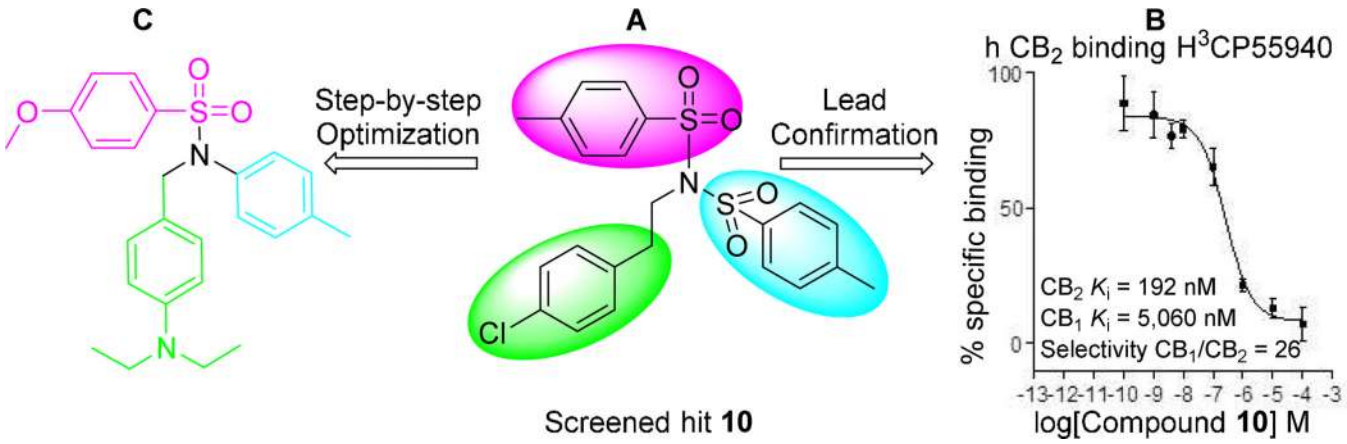

Figure 2.

A novel CB_2 ligand **10** discovered within an *in vitro* high-throughput screening research program and further modified for SAR studies. (A) Lead compound **10**; (B) **10** was validated by [^{3}H]CP-55040 radiometric binding assays showing high CB_2 receptor binding affinity: *K*i = 192 nM and CB_1/CB_2 selectivity (26 fold); (C) Step-by-step medicinal chemistry optimization.

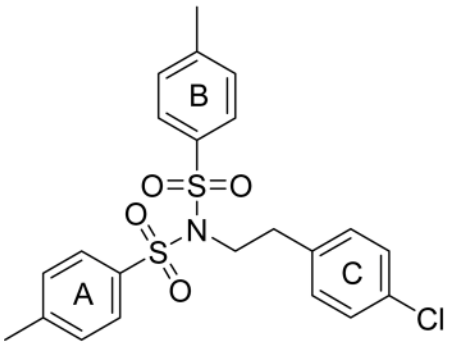

Compound **10**
CB_2 K_i = 192 nM
CB_1 K_i = 5,060 nM
Selectivity CB_1/CB_2 = 26

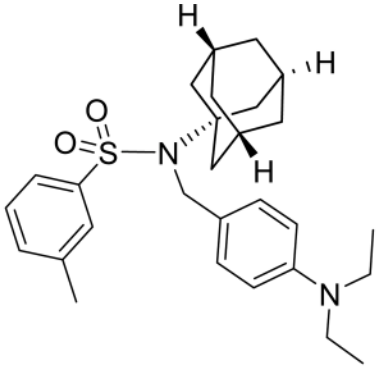

Compound **25**
CB_2 K_i = 19 nM
CB_1 K_i = 8,224 nM
Selectivity CB_1/CB_2 = 432

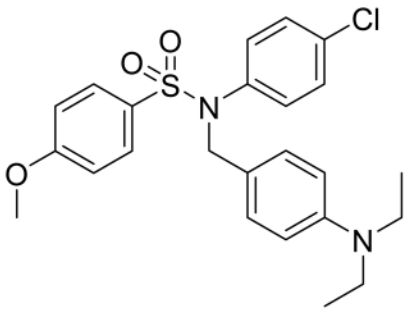

Compound **48**
CB_2 K_i = 14 nM
CB_1 K_i > 20,000 nM
Selectivity CB_1/CB_2 > 1,428

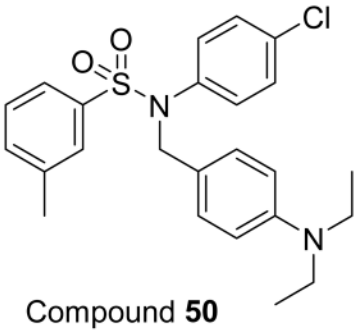

Compound **50**
CB_2 K_i = 2.8 nM
CB_1 K_i = 866 nM
Selectivity CB_1/CB_2 = 309

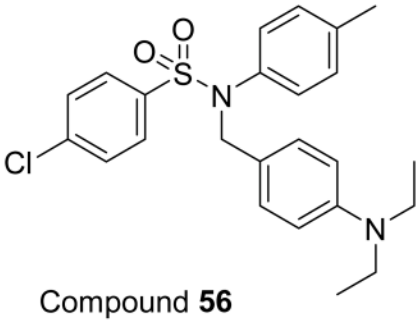

Compound **56**
CB_2 K_i = 3.0 nM
CB_1 K_i = 412 nM
Selectivity CB_1/CB_2 = 137

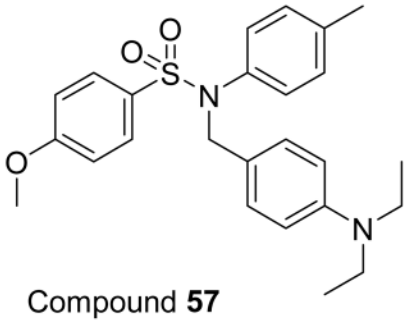

Compound **57**
CB_2 K_i = 0.5 nM
CB_1 K_i = 1,297 nM
Selectivity CB_1/CB_2 = 2,594

Figure 3.
Structures of the lead compound **10** and the modified target compounds **25**, **48**, **50**, **56**, and **57**.

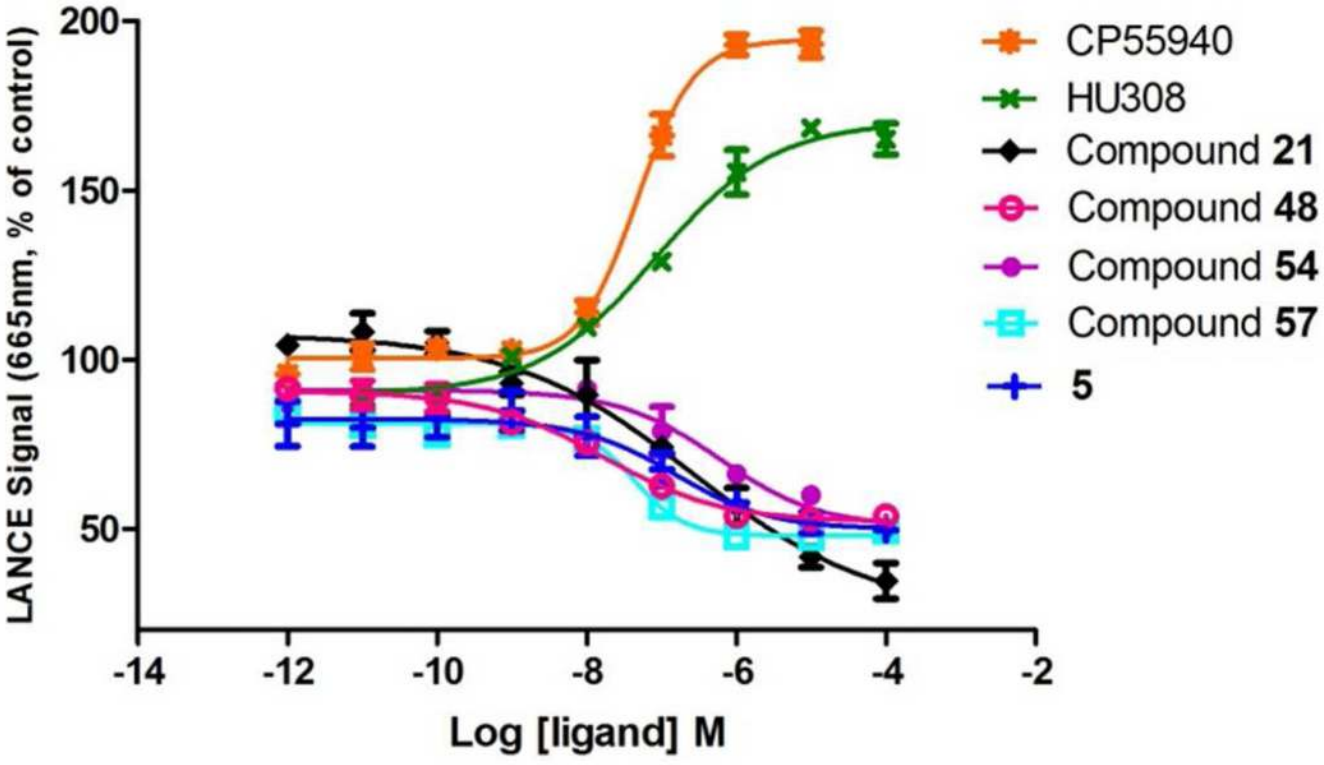

Figure 4.

Comparisons of LANCE signal of different CB_2 receptor ligands in stably transfected CHO cells expressing human CB_2 receptors in a concentration-dependent fashion. EC_{50} values of compounds **21**, **48**, **54**, **57**, and **5** are 268.4 ± 14.5 nM, 16.4 ± 2.84 nM, 608.6 ± 6.06 nM, 42.7 ± 1.35 nM, and 153.8 ± 5.58 nM respectively. EC_{50} for **CP-55,940** and **HU308** are 47.1 ± 3.43 nM and 83.8 ± 5.63 nM. Data are mean ± S.E.M. of all experiments of two or more performed in duplicate or triplicate.

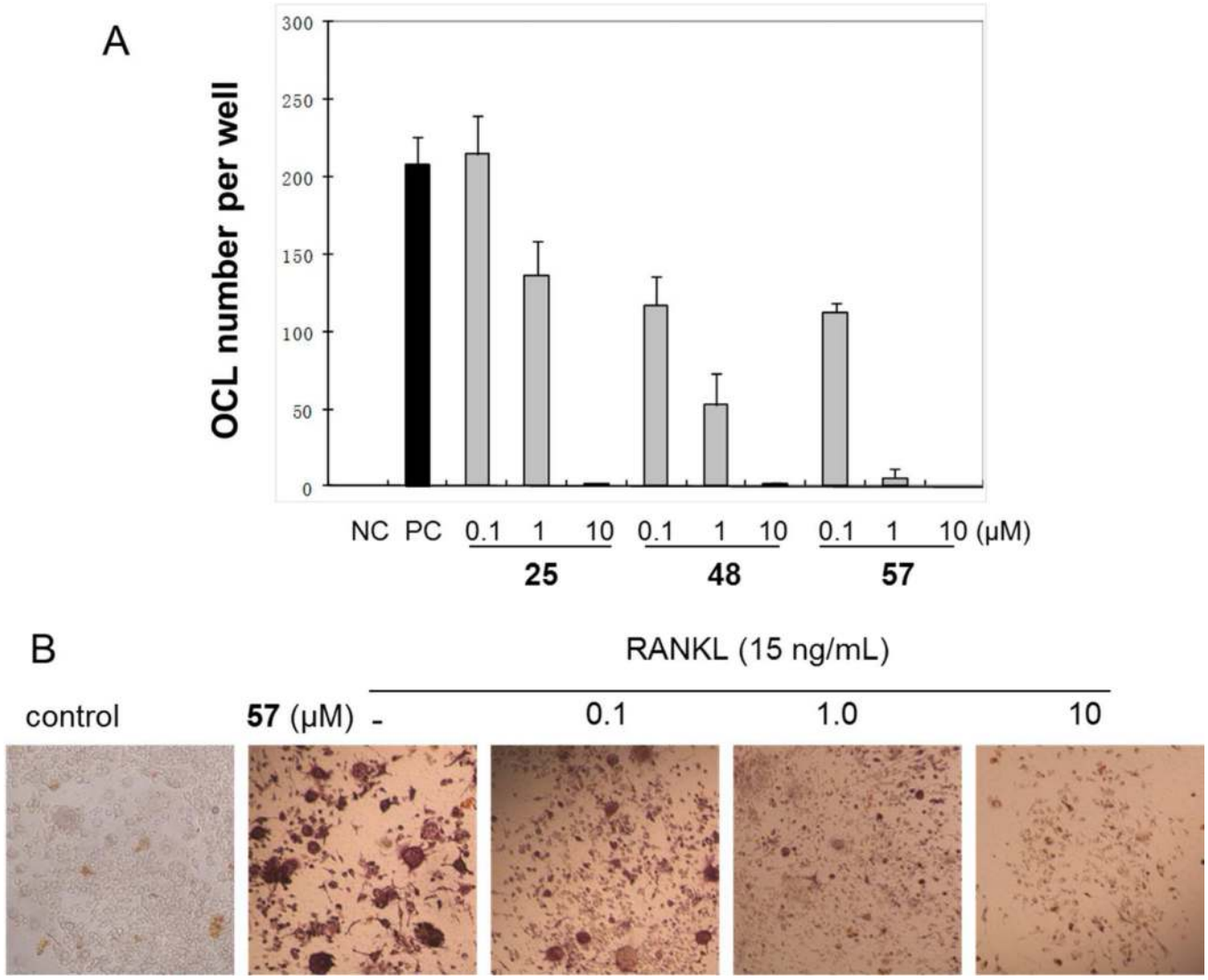

Figure 5.

Anti-osteoclastogenesis activity of top compounds. (**A**) Compounds **25**, **48** and **57** inhibit RANKL-induced osteoclastogenesis in a dose-dependent manner. RAW 264.7 cells (3×10^3 cells/well) were treated with or without RANKL (15 ng/mL), followed by addition of the indicated concentrations of **25**, **48** and **57** for 5 days and stained for TRAP expression. The data are the mean of three experiments carried out in triplicate. The bar indicates the SD. (**B**) Photographs of cells in the test of compound **57** (original magnification 100×).

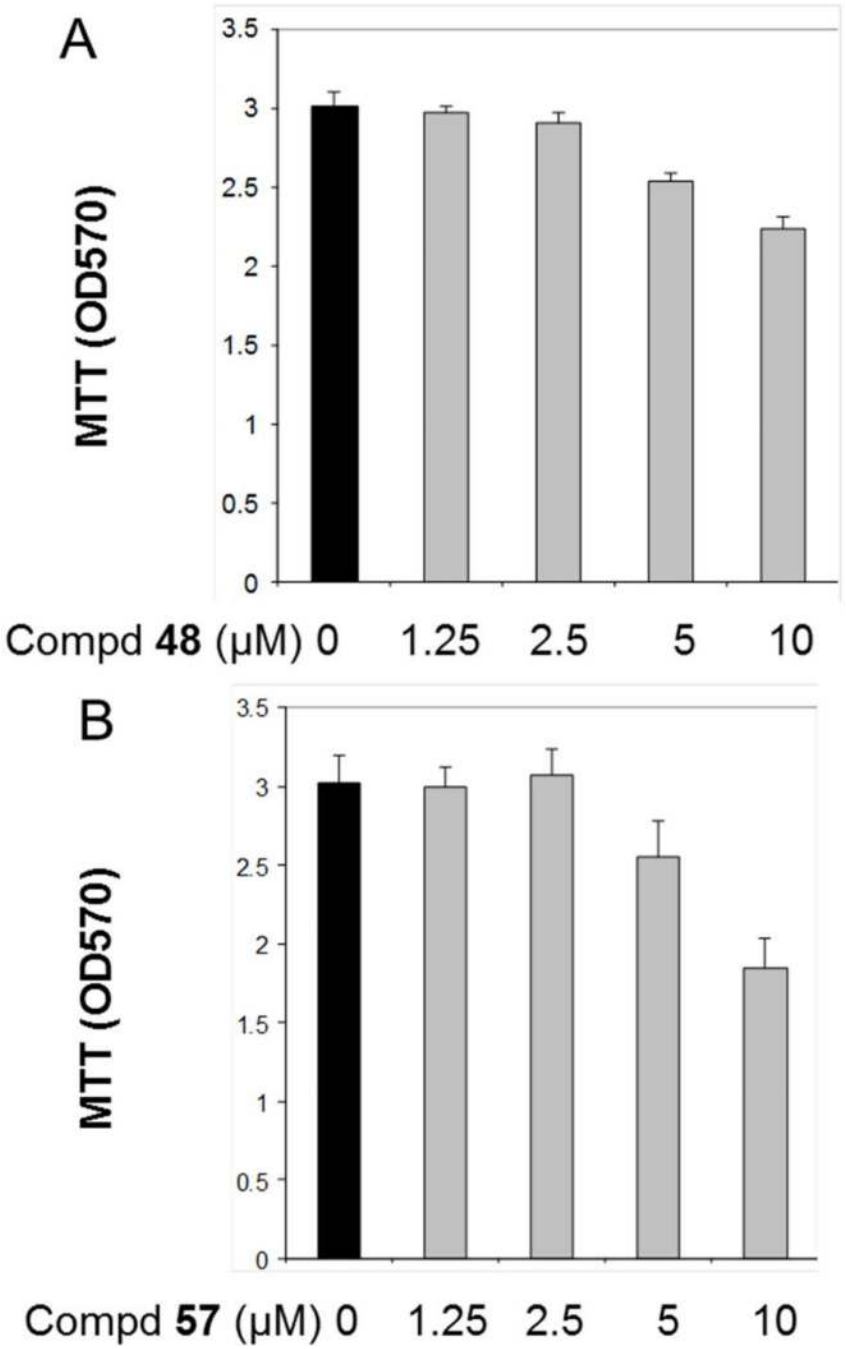

Figure 6.

Cytotoxic effect of top compounds **48** (**A**) and **57** (**B**) on osteoclast precursor. RAW 264.7 cells (3×10^3 cells/well) were plated on 96-well plates. Cells were incubated with the indicated doses of compounds **48** and **57** for 3 days. The percentage of cell survival was determined with the MTT assay. The data are the mean ± S.E.M. of all experiments carried out in triplicate.

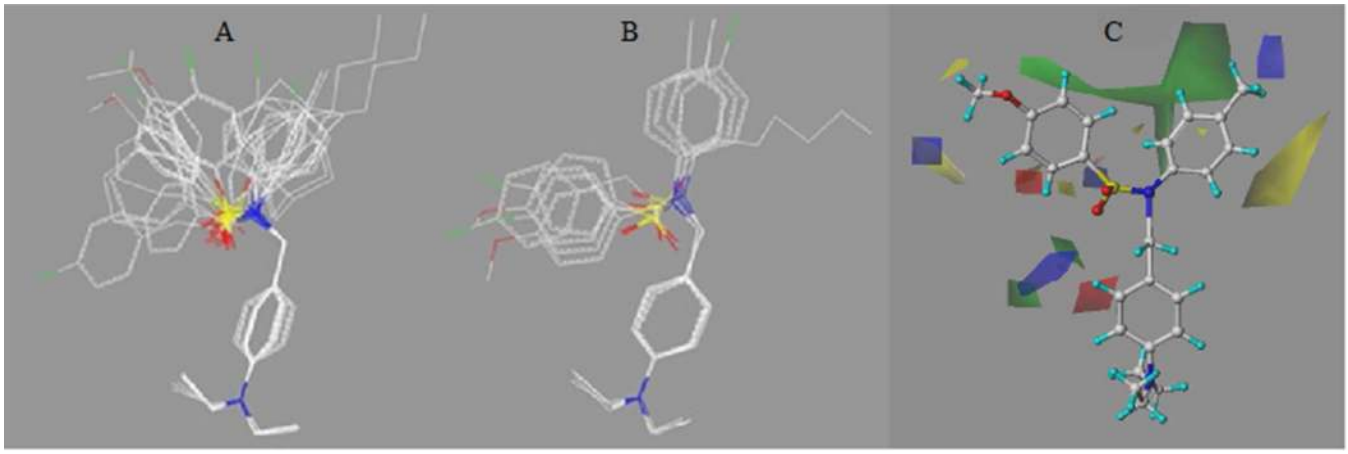

Figure 7.
Overall alignments of training set molecules (**A**) and test set molecules (**B**) to the compound **57** as well as CoMFA contour maps of compound **57** showing steric and electrostatic (**C**) interactions. Sterically (bulk) favored areas are color-coded in green and sterically unfavored areas are in yellow. The red and blue contours reflect whether electropositive or electronegative substituents are favored at a particular position.

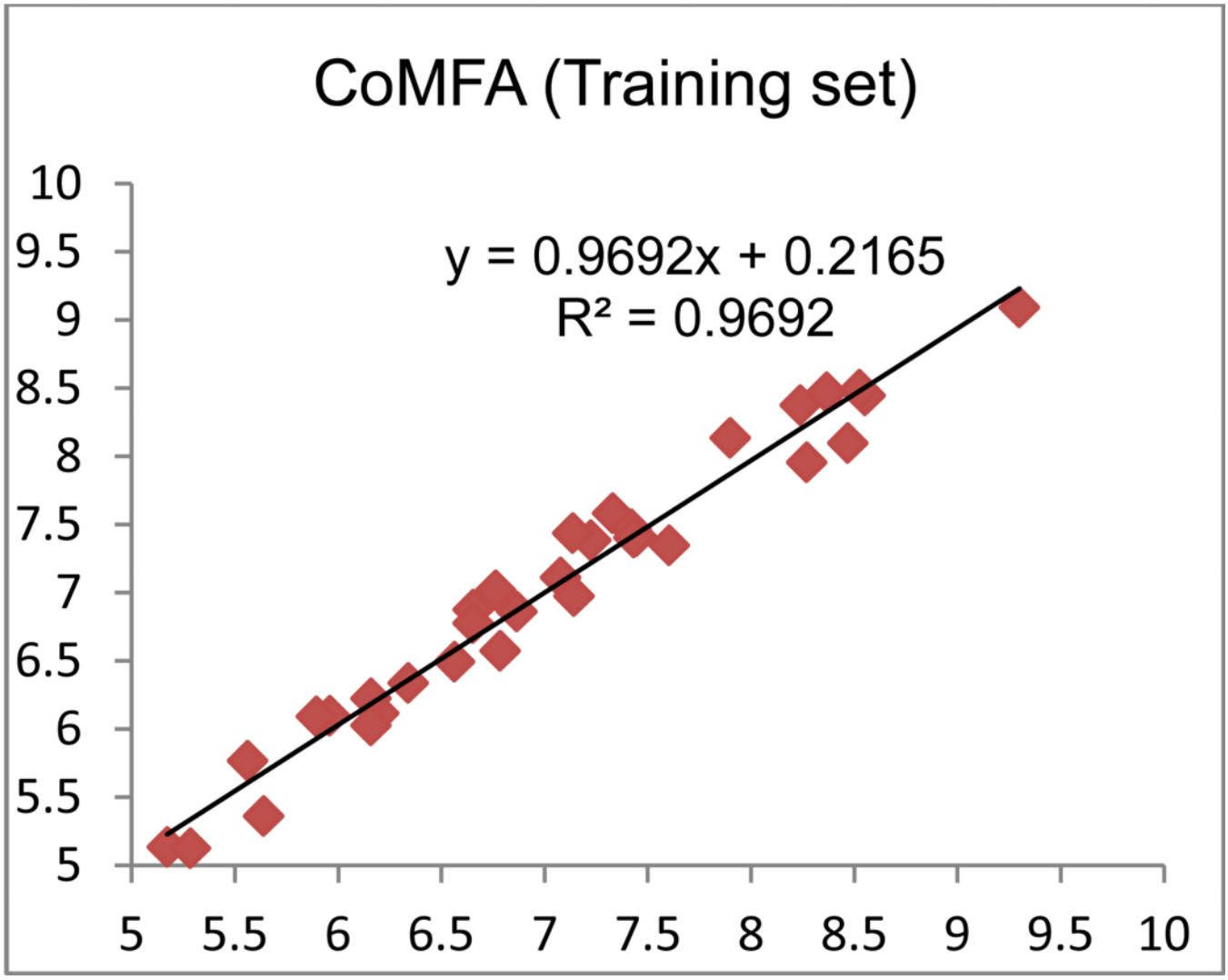

Figure 8.
Plots of CoMFA-calculated and experimental binding affinity values (pK_i) for the training set.

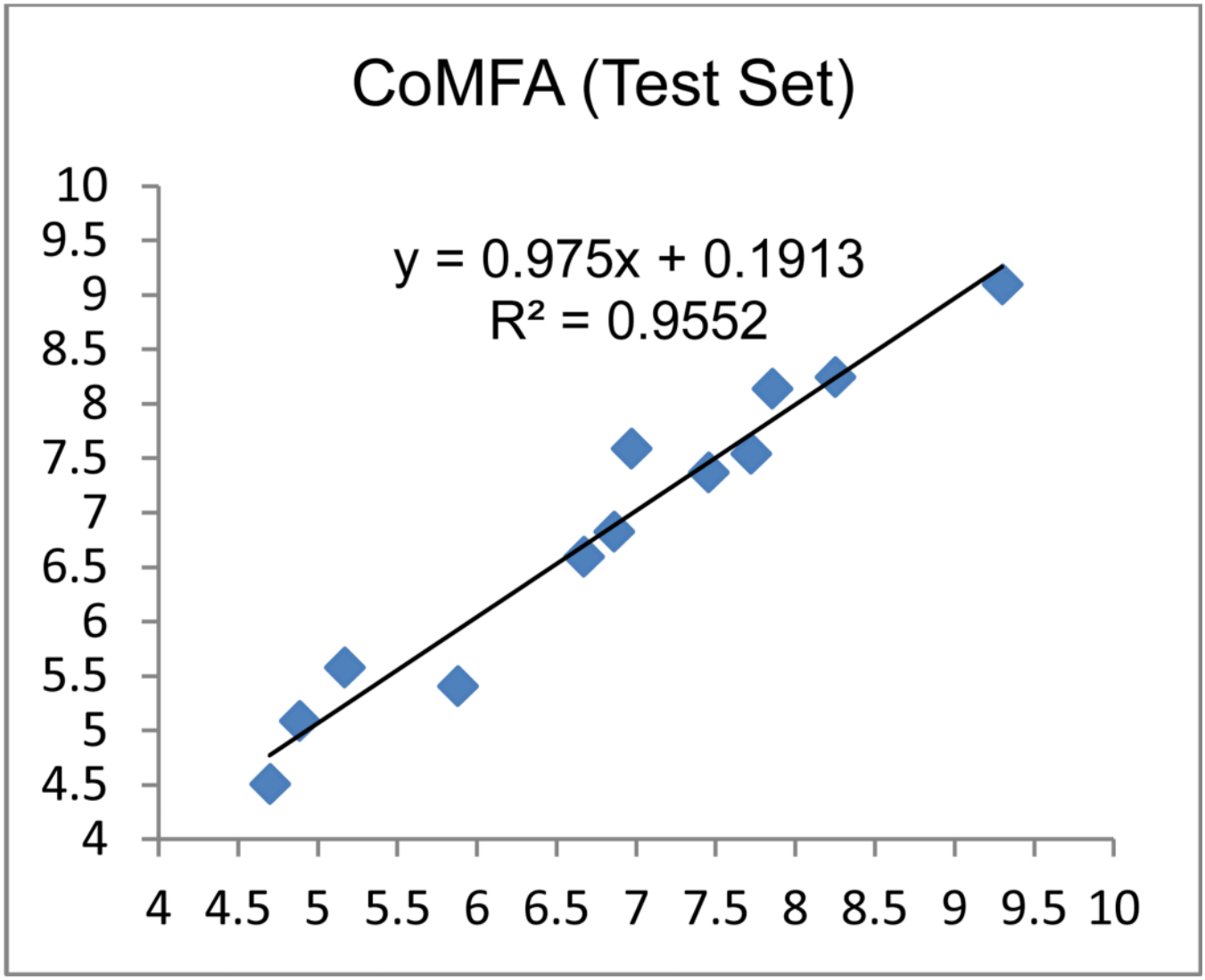

Figure 9.
Plots of CoMFA-calculated and experimental binding affinity values (pK_i) for the test set.

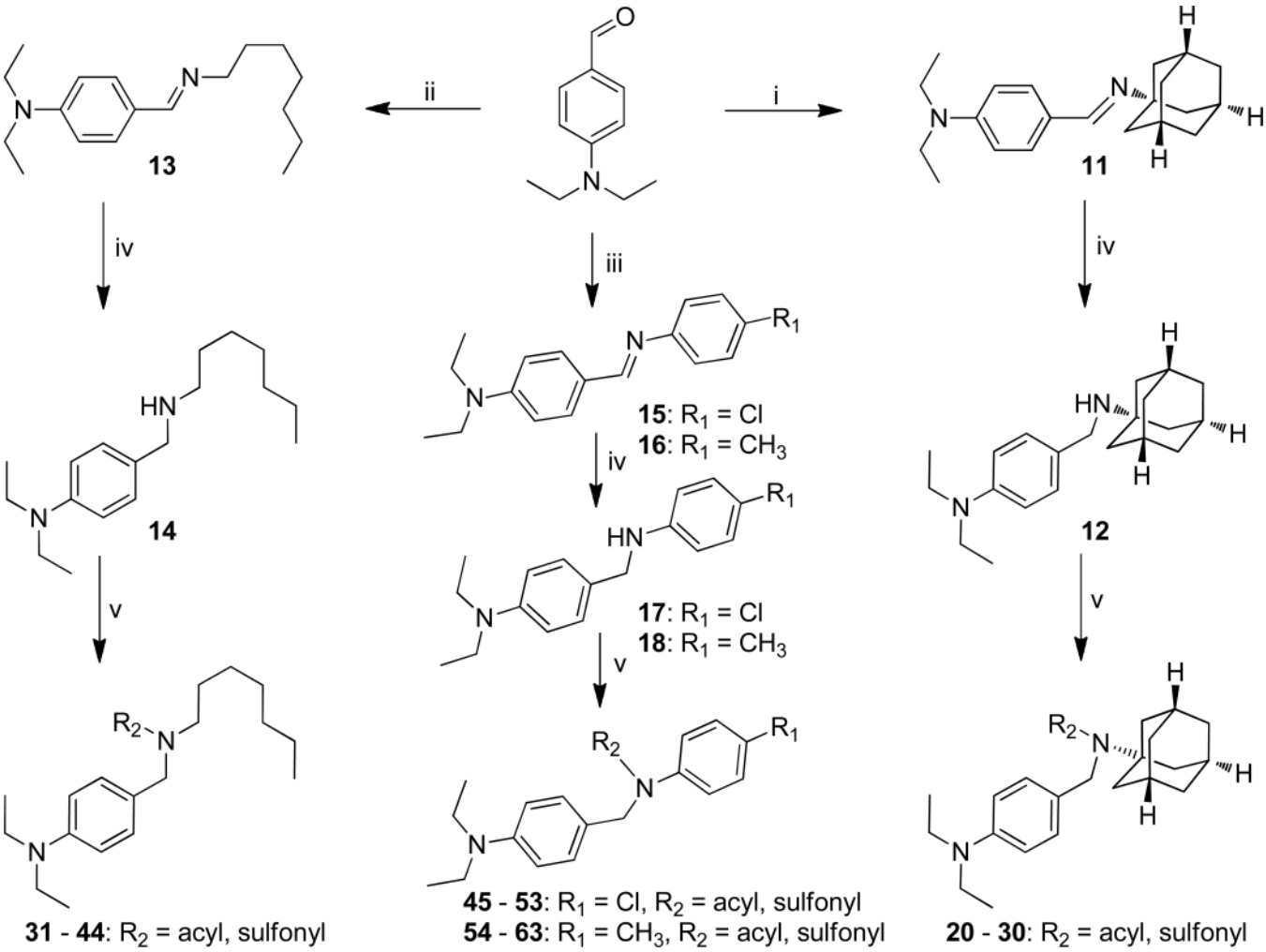

Scheme 1.

General Synthesis of Triaryl Sulfonamide Derivativesa

[a]Reagents and conditions: (i) adamantan-1-amine, methanol, refluxed, 10 h; (ii) heptan-1-amine, methanol, refluxed, 12 h; (iii) *p*-toluidine or 4-chloroaniline, methanol, refluxed, 12 h; (iv) $NaBH_4$, methanol, r.t, 12 h; (v) acyl chloride or sulfonyl chloride, anhydrous DCM, TEA, r.t, 12 h.

Table 1

Radioligand Competition Binding Affinity (K_i) Data for Compounds **12**, **20–30**

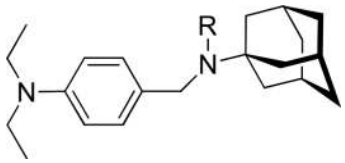

Compd	R	K_i (CB_2), nM[b, c]	K_i (CB_1), nM[a, d]	SI[e]
12	H	19950	NT	
20	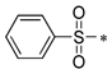	84	11000	130
21	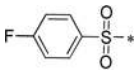	25	4268	170
22	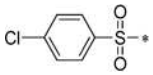	173	2033	11
23	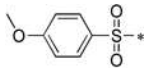	137	7300	53
24	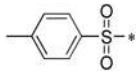	47	NB	425
25	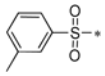	19	8224	432
26	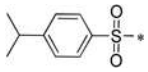	457	NT	
27	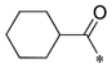	35	NB	> 571
28	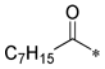	638	NT	
29	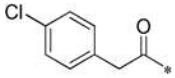	38	NB	> 526
30	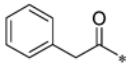	60	NB	> 333
5[f, g]		2.1	NT	
64[f, h]		NT	10.6	

[a, b] Binding affinities of compounds for CB_1 and CB_2 receptor were evaluated using [^{3}H]CP-55,940 radioligand competition binding assay.

[c] NB no binding, K_i > 20000 nM.

[d] NT = not tested.

[e] SI: selectivity index for CB_2, calculated as $K_i(CB_1)/K_i(CB_2)$ ratio.

[f] The binding affinities of reference compounds were evaluated in parallel with compounds **12, 20–30** under the same conditions.

[g] CB_2 reference compound SR144528.

[h] CB_1 reference compound SR 141716.

Table 2

Radioligand Competition Binding Affinity (K_i) Data for Compounds **31–44**

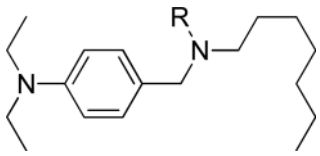

Compd	R	K_i (CB_2), nM[b, c]	K_i (CB_1), nM[a, d]	SI[e]
31	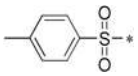	2745	NT	
32	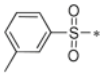	2303	NT	
33	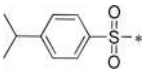	13000	NT	
34	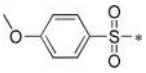	5193	NT	
35	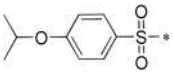	NB	NT	
36	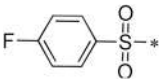	1101	NT	
37	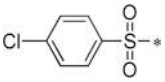	6740	NT	
38	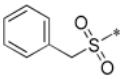	273	NT	
39	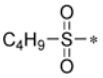	680	NT	
40	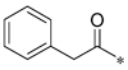	1312	NT	
41	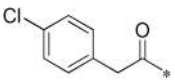	696	NT	
42	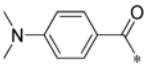	1280	NT	

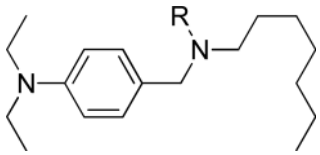

Compd	R	K_i (CB_2), nM[b, c]	K_i (CB_1), nM[a, d]	SI[e]
43	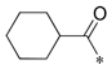	212	NT	
44	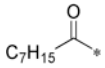	NB	NT	
5[f, g]		2.1	NT	
64[f, h]		NT	10.6	

[a, b] Binding affinities of compounds for CB_1 and CB_2 receptor were evaluated using [^{3}H]CP-55,940 radioligand competition binding assay.

[c] NB no binding, K_i > 20000 nM.

[d] NT = not tested.

[e] SI: selectivity index for CB_2, calculated as $K_i(CB_1)/K_i(CB_2)$ ratio.

[f] The binding affinities of reference compounds were evaluated in parallel with compounds **31–44** under the same conditions.

[g] CB_2 reference compound SR144528.

[h] CB_1 reference compound SR 141716.

Table 3

Radioligand Competition Binding Affinity (K_i) Data for Compounds **17, 45–53**

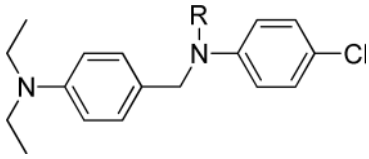

Compd	R	K_i (CB_2), nM[b, c]	K_i (CB_1), nM[a, d]	SI[e]
17	H	6741	NT	
45	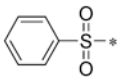	20	1773	88
46	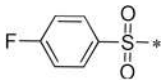	73	1126	15
47	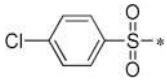	36	6617	183
48	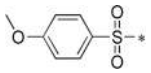	14	NB	> 1,428
49	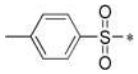	37	137	3.7
50	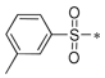	2.8	866	309
51	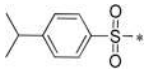	222	NT	
52	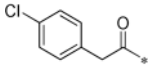	136	NB	147
53	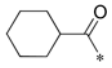	164	NB	121
5[f, g]		2.1	NT	
64[f, h]		NT	10.6	

[a, b] Binding affinities of compounds for CB_1 and CB_2 receptor were evaluated using [^{3}H]CP-55,940 radioligand competition binding assay.

[c] NB no binding, K_i > 20000 nM.

[d] NT = not tested.

[e] SI: selectivity index for CB_2, calculated as $K_i(CB_1)/K_i(CB_2)$ ratio.

[f] The binding affinities of reference compounds were evaluated in parallel with compounds **17, 45–53** under the same conditions.

[g] CB_2 reference compound SR144528.

[h] CB_1 reference compound SR 141716.

Table 4

Radioligand Competition Binding Affinity (K_i) Data for Compounds **54–63**

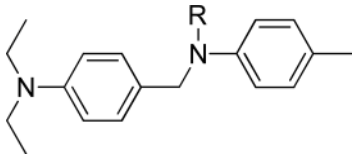

Compd	R	K_i (CB_2), nM[b, c]	K_i (CB_1), nM[a, d]	SI[e]
54	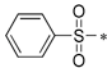	3.4	514	151
55	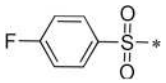	5.6	858	153
56	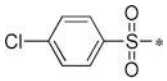	3.0	412	137
57	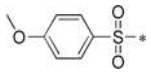	0.5	1297	2594
58	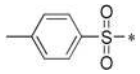	5.4	437	80
59	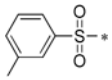	5.8	218	37
60	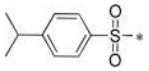	4.3	3365	782
61	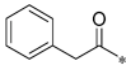	72	NB	> 277
62	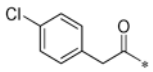	107	3200	29
63	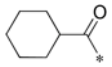	222	202	0.9
5[f, g]		2.1	NT	
64[f, h]			10.6	

[a, b] Binding affinities of compounds for CB_1 and CB_2 receptor were evaluated using [^{3}H]CP-55,940 radioligand competition binding assay.

[c] NB no binding, K_i > 20000 nM.

[d] NT = not tested.

[e] SI: selectivity index for CB_2, calculated as $K_i(CB_1)/K_i(CB_2)$ ratio.

[f] The binding affinities of reference compounds were evaluated in parallel with compounds **54–63** under the same conditions.

[g] CB_2 reference compound SR144528.

[h] CB_1 reference compound SR 141716.

Table 5

Experimental (expt) and Predicted (pred) pK_i Values of Triaryl Sulfonamide Derivatives in the Training Set

Comd	p*Ki* (expt)	p*Ki* (pred)	Residual
17	5.171	5.135	0.0364
20	7.076	7.111	0.0348
21	7.602	7.346	0.2565
22	6.762	7.017	0.2552
24	7.328	7.582	0.2535
26	6.34	6.339	0.0006
28	6.195	6.114	0.0809
29	7.42	7.464	0.0439
30	7.222	7.387	0.1653
31	5.561	5.765	0.2038
32	5.638	5.362	0.2755
34	5.285	5.126	0.1589
36	5.958	6.095	0.1374
38	6.564	6.494	0.07
39	6.157	6.225	0.0684
41	6.157	6.027	0.1298
42	5.893	6.094	0.2011
45	7.899	8.134	0.2352
46	7.137	7.435	0.2975
47	7.444	7.415	0.0288
49	7.432	7.404	0.0282
50	8.553	8.448	0.1055
51	6.654	6.875	0.2209
52	6.866	6.863	0.0027
53	6.785	6.574	0.2113
54	8.469	8.096	0.3727
56	8.523	8.49	0.0326
57	9.301	9.093	0.2077
58	8.268	7.954	0.3137
59	8.237	8.373	0.1364
60	8.367	8.471	0.104
61	7.143	6.973	0.17
63	6.654	6.778	0.1241

Table 6

Experimental (expt) and Predicted (pred) pK_i Values of riaryl Sulfonamide Derivatives in the Test Set

Comd	p*Ki* (expt)	p*Ki* (pred)	Residual
12	4.7	4.509	0.191
23	6.863	6.827	0.0357
25	7.721	7.541	0.18
27	7.456	7.372	0.0843
33	4.886	5.088	0.2025
37	5.171	5.578	0.4071
40	5.882	5.409	0.4729
43	6.674	6.596	0.0781
48	7.854	8.137	0.2828
55	8.252	8.243	0.0094
57	9.301	9.093	0.2077
62	6.971	7.587	0.6157